The role of graphene and its derivatives in modifying different phases of geopolymer composites: A review

R.S. Krishna[1*]; Jyotirmoy Mishra[2]; Bharadwaj Nanda[2]; Sanjaya Kumar Patro[2]; Adeniji Adetayo[3]; Tanvir S. Qureshi[4*]

[1] *Department of Mechanical Engineering, Veer Surendra Sai University of Technology, Burla, 768018, India*

[2] *Department of Civil Engineering, Veer Surendra Sai University of Technology, Burla, 768018, India*

[3]*Department of Chemistry and Biochemistry, Texas State University, 601 University Dr., San Marcos, TX 78666, USA*

[4] *Department of Geography and Environmental Management, The University of the West of England, Bristol, BS16 1QY, UK*

[*]*Corresponding author.*

E-mail address: rskrishna_mtechmda@vssut.ac.in[1], tanvir.qureshi@uwe.ac.uk[4]

Abstract

There is broad agreement among researchers that the next facing of the construction material industry is *'geopolymer composites'*, also called *'green composites*. Although geopolymer composites have been extensively investigated as a new sustainable building material in recent years, their acceptability is still limited owing to few critical fragilities as a commercial material for construction. However, recent progress on geopolymer composites by several scientists suggests that it could be designed at the nanoscale to significantly enhance the chemical and physiomechanical characteristics to overcome multiple limitations. Graphene, a 2D nanomaterial, has been reported to improve various crucial properties when combined with geopolymer composites. This review paper starts with a bibliometric investigation of the studies related to graphene reinforced geopolymer composites (GRGC) to provide useful insights into current research trends. The paper described the synthesis of suitable graphene derivatives and the manufacturing of different phases of GRGC, namely ink, paste, mortar, and composites. Then a critical review is provided on the mechanical and electrical properties enhancement of graphene geopolymer matrix systems through the modification of the composite matrix at the nano-micro structural level. The GRGC has the

potential to be used in multiple applications, such as the recycling of industrial solid waste, and is addressed in this paper. Research gaps were identified in the areas of suitable forms of graphene materials synthesis, dispersion, geopolymer binder type, mixing design, microstructure, and acceptance as well as implementation. The review clarifies those challenging aspects and presents guided solutions for developing sustainable, resilient, and efficient geopolymer matrix-based future materials.

Keywords: Graphene; Geopolymer; Nanomaterials; Composites; Sustainable.

List of Abbreviations

AAM:	Alkali Activated Materials
ALSP:	Alkaline-source particles
ASOP:	Aluminosilicates particles
CNT:	Carbon Nanotube
EPS:	Expanded Polystyrene
GA:	Graphene Additives
GASG:	Graphene reinforced alkali-activated slag-based geopolymer
GGBFS:	Ground granulated blast furnace slag
GN:	Graphene Nanosheets
GNP:	Graphene Nanoplatelets
GO:	Graphene Oxide
rGO:	Reduced Graphene Oxide
GRGC:	Graphene Reinforced Geopolymer Composites
GRSN:	Graphene reinforced slag-based nanocomposite
HGPP:	Hydrated geopolymer particles
LGO:	Large Graphene Oxide
MWCNT:	Multi-walled Carbon Nanotubes
OPC:	Ordinary Portland Cement
POFA:	Palm Oil Fuel Ash
SF:	Silica Fumes
SGO:	Small Graphene Oxide
WEA:	Waste EPS beads in AAMs (Alkali Activated Materials)

1. Introduction

Advanced sustainable construction materials are highly desirable in the infrastructure industry. This is particularly owing to the confinements of many of today's most utilized construction materials' impact on the environment. In order to meet the requirements for emerging construction applications, desirable construction materials are required to meet

enhanced durability and mechanical efficiency that must incorporate multiple functionalities. While the geopolymer composites are showing great prospects to be the sustainable green composite for the construction industry, advanced 2D graphene-based nanomaterials may have an effective role in overcoming different challenging aspects of these alternative composite systems.

The multi-disciplinary field of nanotechnology has witnessed an increasing number of interests in research, journal articles, patents, and applications over the last decades. This growth was primarily due to research & innovation by researchers to better understand the matter, their interactions at the molecular level, and find ways to modify them to yield bulk materials of desired properties. Nanomaterials as additives in cementitious materials have led to amelioration of the mechanical properties, hydration process, and microstructure of such composites [1,2].

It is widely recognized that in the construction industry, Ordinary Portland Cement (OPC) contributes about 6 – 9% of world CO_2 emissions per year [3]. The production of OPC also consumes a considerable amount of natural resources and energy. A stringent control of pollution in the traditional cement manufacturing industry could mitigate the negative environmental impact. Continually, scientific research and industrial companies have been pressured by the increasing environmental impact, to invest in energy-saving and environmentally friendly cement alternatives.

'Geopolymers' (inorganic aluminosilicate polymers) based binder system has attracted global attention over a short time period. This is due to geopolymer composites' high sustainability and potential as an alternative to OPC-based concrete and composite system. Major precursors for geopolymer composites are large industrial waste products such as fly ash and slag. Hence, the synthesis of geopolymer composite reduces reliance on the use of virgin materials, fostering a circular economy and sustainability [4]. Geopolymer composite has an

extremely low carbon impression, with up to 80% lower CO_2 discharge as oppose to OPC [5]. Besides environmentally cleaner production factors, geopolymer composite is cost-effective, chemically stable, corrosion-resistant, can be designed to gain rapid strength, results in a low rate of shrinkage, freeze, and thaw resistant, as well as outstanding thermal properties [6,7]. Chemical stability indicates the leaching behavior of geopolymer composites whereas corrosion-resistant indicates its resistance to aggressive solutions such as acids, seawater, and sulphate solutions. A geopolymer composite binder has the potential to be used in various building materials, such as fire safety coatings and composites of reinforced and unreinforced concrete [8]. Due to the increasing demand for sustainable and alternative of OPC-based concrete in the construction industry, geopolymer composites showing high potential to be an eco-friendly, cost-efficient, and high-performance construction material. Geopolymer composites could be efficient and at par with conventional building materials.

Geopolymer composites are produced through a reaction between precursor materials composed of aluminum and silica such as metakaolin [9], slag [10], fly ash [11], silica fume [12], red mud [13], mine tailings [14,15], ferrochrome ash [16], etc. and alkaline activator solution which can be a mixture of sodium hydroxide and or sodium silicate [17]. Acidic phosphates are also studied as an activator in the synthesis of geopolymer composites [18].

Despite being a high potential green binder system, pure geopolymers face challenges due to their low flexural and tensile strength in combination with other defects such as brittleness and poor impermeability [19,20]. Defects in pure geopolymer may arise due to existing cracks inside the geopolymer matrix, and its inherent porosity resulted from the inorganic bond formation during geopolymerization [20,21]. These limitations have restricted geopolymer composites' wide adoption for structural applications [22], which led to the necessity of adding secondary reinforcement particles, i.e., nanoparticles into the geopolymer matrix to account for the deficits. Various efforts have been made in this field using carbon-

based nanomaterials such as carbon nanotubes, GO, rGO, and graphene nanoplatelets (GNP), due to their superior property enhancing characteristics [23,24].

Recent studies have displayed effective utilization of graphene, a distinctive two-dimensional carbonaceous nanomaterial as a reinforcement agent for geopolymer matrix. The use of graphene-based materials at low loading (<1%) has shown improvements in the microstructural and flexural strength of geopolymer composites, and reduction in porosity due to strong bonding and mechanical interaction between graphene and geopolymer matrix [25–28]. Studies by Saafi et al. [27,29–31], Ranjbar et al. [19], Yan et al. [32,33], and Zhang et al. [34–37], have significantly contributed and highlighted the property enhancing tendency of graphene in AAMs and geopolymeric matrix systems.

Exceptional properties of graphene include theoretical surface area (single layer graphene) close to 2630 m^2g^{-1}, the electrical conductivity of 10^6-10^7 Sm^{-1} (isolated single graphene particle), the ultimate tensile strength of 130 gigapascals, the density of 2.267 gcm^{-3}, with excellent flexibility, high optical transparency (~97.7%), excellent chemical stability, excellent gas impermeability and 3000 - 5000 $Wm^{-1}K^{-1}$ thermal conductivity at room temperature; which have accounted for its universal interest [38–46]. Therefore, the development of exceptional geopolymer composites formed through the inclusion of graphene and its derivatives such as GO and rGO is indicative of advancement towards the development and use of graphene reinforced geopolymer composites (GRGC) for wide structural applications. Fig 1 presents the use of different materials and processes in developing different phases of GRGC systems such as ink, paste, and aggregate-based. GRGC holds the potential to unlock several closed doors in the field of interdisciplinary research and had demonstrated promising results in mechanical strength enhancement, oxidation degradation of dyeing wastewater [34], extrusion-based 3D printing of nanocomposite structures [47], multifunctional structural supercapacitor [48], superionic

conduction for structural health monitoring [27], production of H_2 as a photocatalyst by solar photo-reduction [37], etc. Zhang et al. [34,37] developed a novel bottom ash-based GRGC for photocatalytic production of H_2 and oxidation degradation of dyeing wastewater, whereas, Zhong et al. introduced GRGC in 3D printing applications [28].

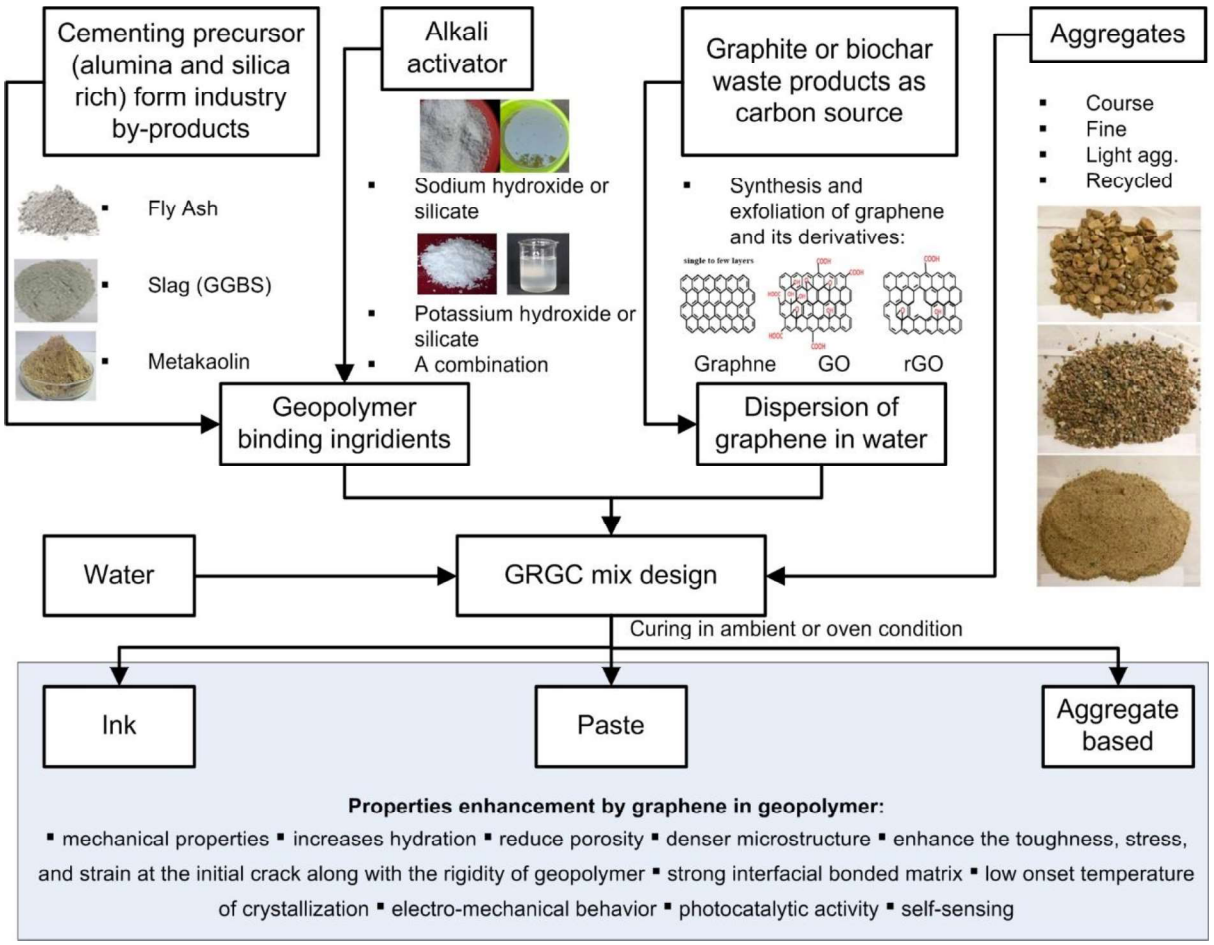

Fig. 1. Schematic of the graphene reinforced geopolymer composite systems.

This study includes a bibliometric analysis to investigate the past works associated with GRGC and recognize the current research trends. The review presents the synthesis and characterization of most up to date graphene derivatives used in GRGC system, such as pristine graphene, GNP, GO, rGO, and hybridized graphene. There are three major GRGC phases, that is ink based GRGC, paste based GRGC, and aggregate based GRGC, which are effectively described with the mixing process identifying existing research challenges and potential applications. Despite the tremendous propitious results obtained from several

observations, to the best of the authors' knowledge, adequate numbers of investigations have not been performed to evaluate the reaction mechanisms and compatibility of graphene derivatives in different geopolymer binders' hydration systems (i.e., ferrochrome ash, rice husk ash, etc.), which has also been discussed. Existing investigations have mostly emphasized the mechanical properties of GRGC (i.e., compressive strength, flexural strength, flexural toughness, fracture toughness, etc.), which provides tremendous scope for further studies on different phases of GRGC. Therefore, this study is focused on unraveling such research gaps in the field of GRGC while reviewing its past and current developments.

2. Bibliometric Analysis

The past couple of years have witnessed a tremendous rise in research on GRGC due to its remarkable properties in diverse application scenarios. Bibliometric analysis is effective in generating datasets that can be used by policymakers, researchers, and other stakeholders for improving the quality of research [49]. The objective of this analysis is to study the research and development towards GRGC in terms of bibliometric maps and research trends through the use of open-source VOS Viewer software.

The Scopus database was utilized to obtain information on the GRGC. A total number of 80 articles were found in the Scopus database, with the keywords "Graphene, Geopolymer, Geo-Polymer, Geopolymeric and Geopolymerization" accessed on June 8, 2021. The articles ranged from the year 2014 to 2021. Sample articles were downloaded in *.csv format and were further compiled into a single file to be analyzed by the VOS Viewer software. The software is used to analyze and visualize trends in the form of bibliometric maps [50].

The software offers 5 types of bibliometric analysis among which are co-authorship, co-occurrence, citation, bibliographic coupling, and co-citation. However, co-occurrence analysis was used in the study to investigate the co-occurrence of sample article keywords (i.e., including both index as well as author keywords) and to identify prominent keywords

reflecting the research trends. The threshold for the co-occurrence of keywords has been set at 3; if the keywords have been at least used thrice in different articles. Fig 2 shows the density visualization; revealing the depth/density of the analyzed keywords in each cluster. It illustrates the close relationship between different clusters. The keywords in each cluster of the network visualization are replaced by prominent keywords. Keywords were labeled with different colored circles and the size of the circle is positively correlated with the appearance of keywords in the sample articles. Therefore, the size of the letters and circles was determined by the frequency of occurrence. After being analyzed, 4 clusters were formed (Blue, Green, Red, and Yellow,) in Fig. 2; indicating the relationship between one topic and another. Different bibliometric mapping visualizations can be obtained through the software.

After reviewing several articles on GRGC, the authors have hypothesized specific prominent research trends (i.e., structural materials, hydrogen production, mechanical properties, and microstructural characterization) in Table 1, through the assessment of the analyzed keywords in the network and density visualization. The apparent use of geopolymer composites in the construction industry is evolving gradually while promoting the investigation of advanced composites such as GRGC, owing to their enhanced mechanical and electrical properties. Photocatalytic hydrogen production with the help of GRGC is a relatively novel application that exhibits the multifaceted utilization of the composite. Clearly, graphene-based materials such as GO and rGO are used targeting to improve the geopolymerization, hydration kinetics, mechanical properties (compressive and flexural strength, fracture toughness), photocatalytic performance, and microstructure of the geopolymer composites. The research trends are considered during the following review.

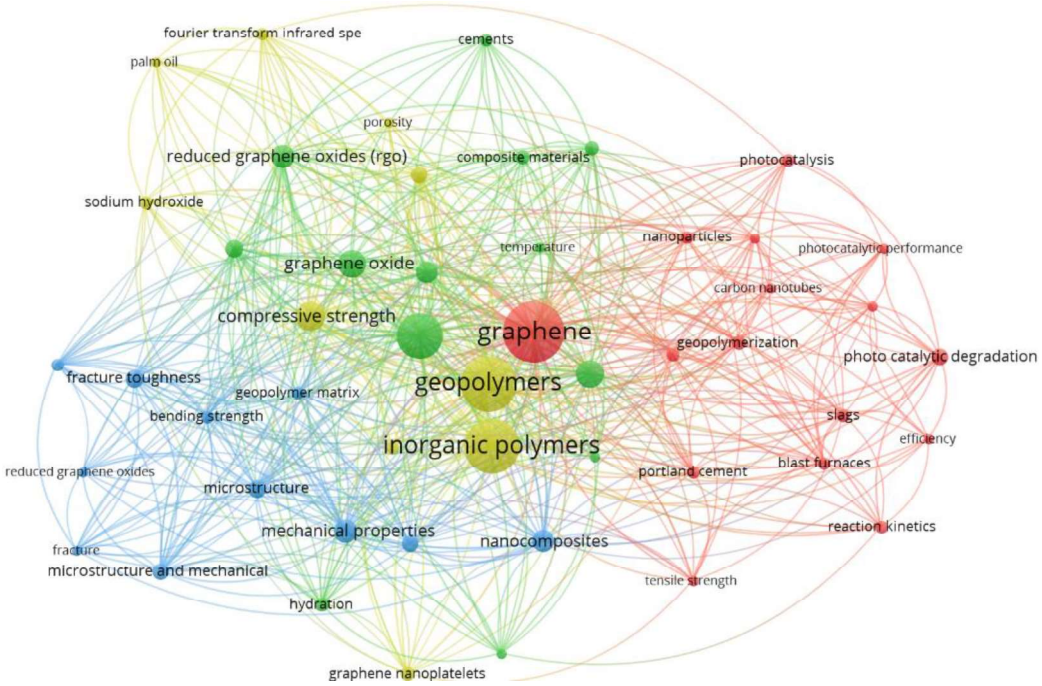

Fig. 2. Network visualization of keywords.

Table 1. Prevalent research trend assessment.

Research Trend	Keywords
Structural Materials	Cements, Porosity, Composite materials, Sodium Hydroxide, Temperature, Geopolymerization, Geopolymer matrix, Geopolymers, Slags, Efficiency, Blast furnaces, Portland cement, Hydration
Mechanical Properties	Compressive strength, Fracture toughness, Bending strength, Mechanical properties, Tensile strength, Fracture
Microstructural Characterization	FTIR, rGO, GO, Nanoparticles, Graphene, Carbon Nanotubes, Inorganic polymer, Microstructure, Nanocomposites, GNP
Hydrogen Production	Photocatalysis, Photocatalytic performance, Photocatalytic degradation

3. Synthesis of Graphene and Graphene Derivatives

Carbon exists in various allotropic forms and colors. Graphene, a single layer of bonded carbon atoms derived from a graphite matrix structured in a 2-dimensional (2D) hexagonal lattice, is one of its most important allotropes. Graphene is capable of being wrapped up to form a spherical structure of 0-dimensional (0D) fullerene (Buckyball), rolled to form a cylindrical structure of 1-dimensional (1D) carbon nanotube (CNT), and assembled into

several layers to produce 3-dimensional (3D) graphite structure as illustrated in Fig. 3. The significant need for graphene as a promising reinforcement material for the manufacture of composite materials is due to its exceptional characteristics.

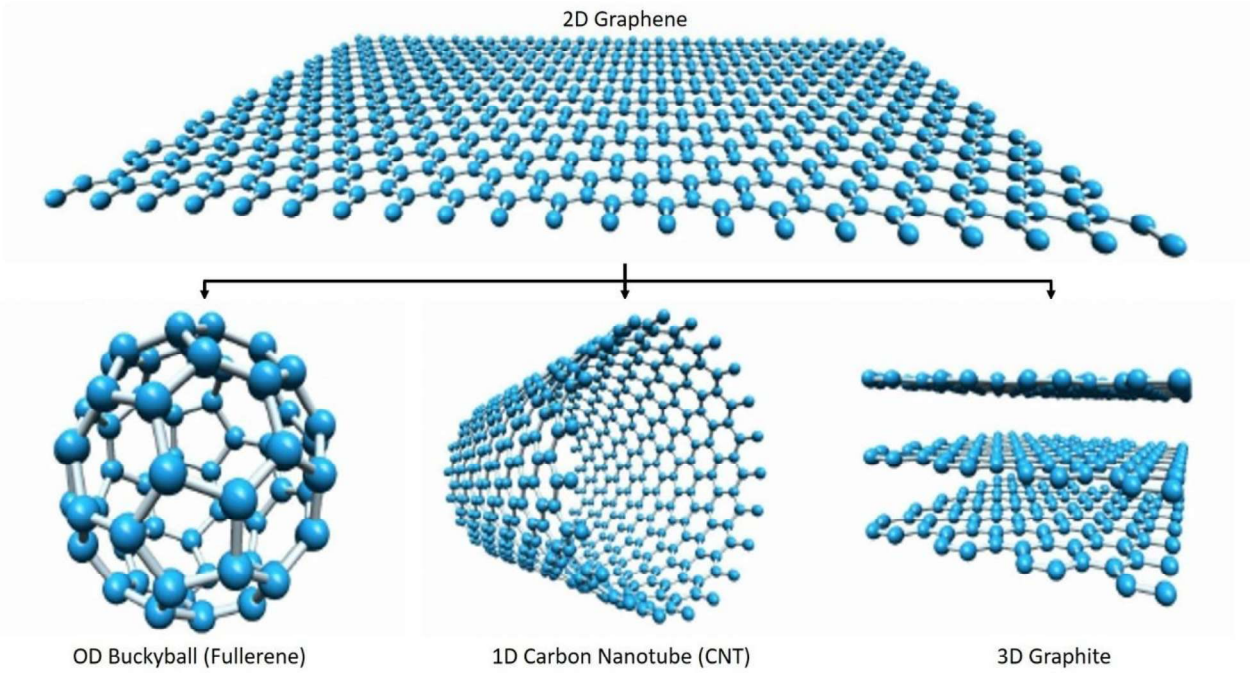

Fig. 3. Illustration of carbon allotropes with 2D graphene as a building block for other dimensions [51].

The wide adoption of graphene derivatives in research has been due to continuous efforts being made for low-cost industrial-scale production combined with high quality and faster processing which provides an opportunity for the advancement of graphene reinforced geopolymer composites. Various works of literature on graphene synthesis techniques and applications of graphene have been reviewed in the paper [52,53]. The different techniques comprise mechanical exfoliation, liquid-phase exfoliation, chemical and organic synthesis, epitaxial growth, and chemical vapor deposition (CVD). In a study by Tang et al. [54], various approaches/methods have been developed to synthesize graphene and its derivatives. Each technique has its share of advantages, disadvantages, and cost-effectiveness. Currently, GNP, GO, and rGO, are the most investigated graphene derivatives used as nanofiller

graphene additives (GA) for geopolymer composite properties enhancement [31]. While very recently hybridized graphene is also studied to improve geopolymer composite.

3.1. Pristine and Graphene nanoplatelet (GNP)

CVD is a commonly used method for the synthesis of pristine graphene films [55]. However, the CVD method lacks industrial scalability and faces cost constraints, which is possibly the major bottleneck in graphene commercialization and application in bulk quantities required for geopolymer. GNPs can be separated from graphite in aqueous solutions through sonication, accompanied by an oxidation-reduction process [56]. The key issue here is the presence of excessive structural defects within the graphene lattice, even after the reduction. In contrast, liquid-phase exfoliation was demonstrated to offer a scalable and cost-effective route to produce high-quality, unoxidized GNP from powdered graphite [57]. The high-shear liquid exfoliation can achieve the exfoliation in liquid volumes from hundreds of milliliters up to hundreds of liters and beyond [58].

3.2. Graphene Oxide (GO)

Graphene oxide (GO) is typically synthesized from graphite precursors [59] through improved or modified chemical exfoliation methods: the Brodie method [60], Staudenmaier method [61], and Hummers method [62] depending on their oxidizing agents as shown in Fig. 4. However, the oxidation reactions involved in the synthesis process tend to be explosive, emitting harmful and toxic gases (NO_2, N_2O_4), which obstructed its large-scale production. A report by Marcano et al. expounded an improved and green method (the Tour method) for synthesizing GO in which the oxidation process was refined by increasing $KMnO_4$ content and eliminating $NaNO_3$ [63]. This encouraged scientists and researchers to discover more economically friendly synthesizing methods for the production of GO. Produced GO structure yields oxygen-containing functional groups such as hydroxyl (-OH), epoxy (C-O-

C), and carboxyl (-COOH). The presence of these hydrophilic functional groups promotes good dispersion in aqueous solvent for application as additives in geopolymer materials [64].

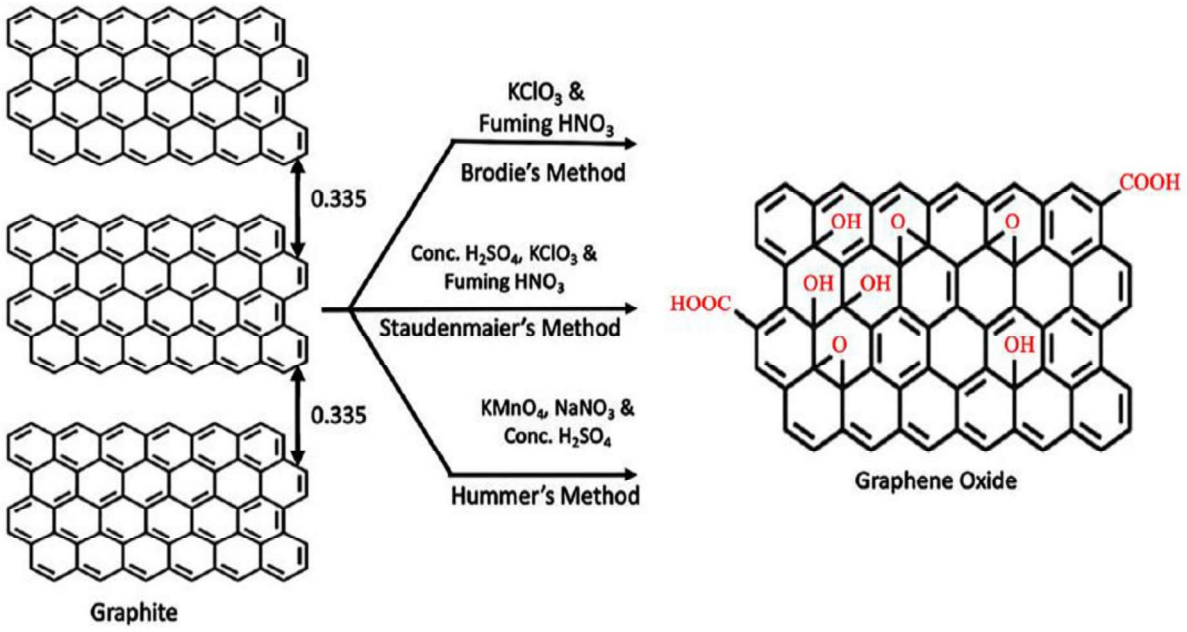

Fig. 4. Common chemical oxidation routes to Graphene oxide preparation [52].

A summary of current research, observations, findings & methods on the synthesis of GO has been illustrated in Table 2. However, GO faces some very crucial challenges such as low electrical conductivity and limited chemical, thermal or mechanical stability.

Table 2. Current developments and major findings by various researchers in synthesizing different forms of GO.

Ref	Desired Material	Ingredients		Method	Major Findings
		Graphite Precursor	Oxidizing Agents & Chemicals		
Yu et al. 2016 [65]	GO	Natural Flake Graphite	K_2FeO_4+KM_nO_4 + H_3BO_3+ H_2SO_4+DI Water + H_2O_2	Modified Hummers	Synthesis of GO through modified $NaNO_3$-free Hummer's methods based on a one-pot synthesis routine.
Muzy	Graph	Scale,	H_2SO_4+NaN	Hummer	Tour's method is more effective

ka et al. 2018 [66]	ite Oxide	Flake, Synthetic Graphite	O_3+ KM_nO_4 + H_3PO_4+KNO_3	s, Modified Tour	for introducing oxygen into the graphite structures & synthetic graphite is least susceptible to oxidation while flake graphite being the most.
Pei et al. 2018 [67]	GO Sheets	Flexible Graphite Paper	H_2SO_4	Electrochemical	Synthesizing GO by continuously introducing graphite intercalation compound paper (GICP) into dilute H_2SO_4.
Ranjan et al. 2018 [68]	GO Foam	Graphite Flakes	H_2SO_4+ H_3PO_4+HCL + H_2O_2+DI Water+ KM_nO_4	Modified Hummers	Elimination of the explosive nature of the underlying reactions yields good quality GO.
Piñas et al. 2019 [69]	Graphene Sheets	Graphite Flakes	(Fe2+/H_2O_2) + H_2SO_4 + H_2O_2 + DI Water + HCL	Fenton reagent chemistry	Large-scale graphene production by Fenton reaction- (a mixture of Fe^{2+}/H_2O_2) assisted the exfoliation process.
Habte and Ayele 2019 [70]	GO	Graphite Powder	(H_2SO_4/H_3PO_4) + $KMnO_4$+ DI Water+H_2O_2 + HCL+ $BaCl_2$	Tour	Production of GO without emitting toxic gases through a combination of H_2SO_4/H_3PO_4 (9:1 volume ratio).

3.3. Reduced Graphene Oxide (rGO)

Reduced graphene oxide (rGO) is processed from graphene oxide (GO) to aid dispersion and the use of reducing agents through the sonification of GO to eliminate oxygen-containing functional groups and form rGO as illustrated in Fig. 5(a). The reduction techniques include the chemical reduction [71], thermal reduction [72], microwave & photoreduction [73,74], photocatalyst reduction [75], solvothermal/hydrothermal reduction [76,77], acid/alkali [78], and other treatments such as laser [79], plasma [80], electrochemical [81], and two-step reduction [82]. During the electrochemical reduction of GO by Pfaffeneder-Kmen et al., the carboxylate group was reduced to carbonyl (C-O) with a few residual oxygen-containing groups which are beneficial for the dispersion in the geopolymer matrix [83]. In work by Liu et al. [84], GO was reduced in a strong alkaline solution, while reducing the oxygen

functional groups as stated through the Fourier-transform infrared spectroscopy (FT-IR) curves of GO & rGO; Fig. 5(b).

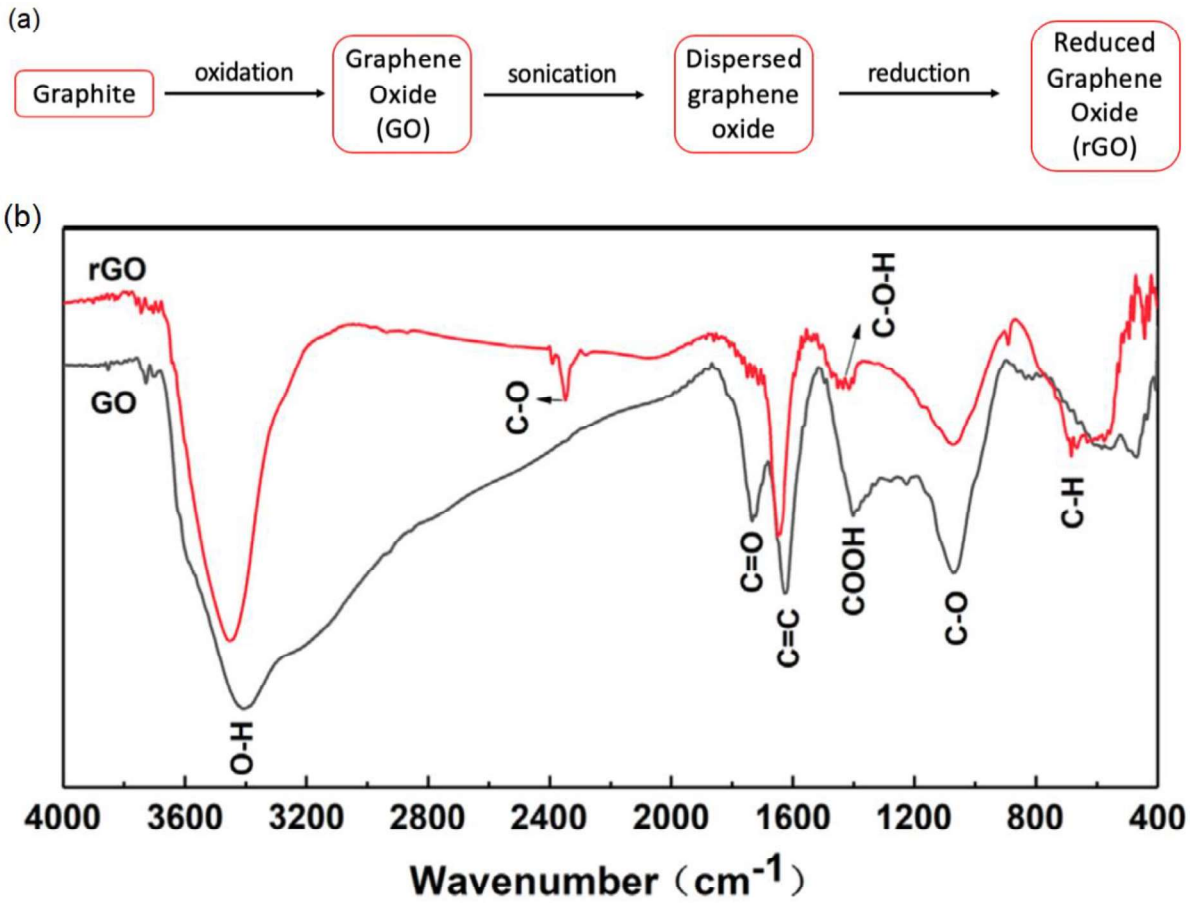

Fig. 5. (a) Synthesis of reduced graphene oxide (rGO) from starting graphite material, (b) FT-IR spectra of GO and rGO [52,84].

According to Pei and Cheng, the elimination of functional groups of oxygen and atomic-scale lattice defects that adversely affect GO's electrical conductivity concludes in the recovery of the graphitic lattice conjugate network and electrical conductivity improvements to yield reduced graphene oxide (rGO) closer to pristine graphene [75]. Several reducing agents have been used such as norepinephrine [85], polyelectrolyte [86], sodium citrate [87], Ethylenediamine (EDA) [88], sodium borohydride ($NaBH_4$) [89], hexamethylenetetramine [87], hydroquinone [90], aluminium powder [91], etc. Due to the negative impacts of some of the reduction process which includes toxic reducing agents and by-products, new age

scientists and researchers have been developing green and eco-friendly methods for large-scale synthesis of rGO [92]. This newly developed green technology includes biomolecules such as vitamins, enzymes, amino acids, alkaloids, alcoholic derivatives, and many others [93]. Table 3 provides a short overview of the current and past developments in the field of synthesizing rGO.

Table 3. Current developments and major findings by various researchers in synthesizing different forms of rGO.

Ref	Desired Material	Ingredients		Method	Major Findings
		Graphite Precursor	Reducing Agents		
Iravani 2011 [94]	rGO Sheets	GO Sheets	Hydroxylamine	Chemical Reduction	Chemically reduced graphene oxide using hydroxylamine as a reductant.
Zhou et al. 2011 [95]	rGO	Graphite Oxide	Nitrogen	Thermal exfoliation & reduction	rGO from flake graphite acquired the highest degree of reduction with the fewest defects when compared with rGO's obtained from scale and synthetic graphite.
Muzyka et al. 2018 [66]	rGO	GO	Hydroiodic acid (HI)+ Epigallocatechin Gallate (EGCG)	Two-Step reduction	rGO sheets were useful in eliminating oxygen-containing functional groups in GO to obtain rGO, with the use of reductants such as HI sheets and EGCG.
Ahmed et al. 2018 [96]	rGO powder	GO powder	Green Tea Extract	Conventional stirring followed by centrifugation & ultrasonication	rGO using green tea extract as the reducing agents by manipulating their reaction time.
Tai et al. 2018 [97]	rGO Platelets	Graphite Oxide	Ascorbic acid	Chemical Reduction	rGO production by the previous oxidation of graphite with a Fenton reagent.

Piñas et al. 2019 [69]	rGO	GO	Ascorbic acid	Chemical Reduction	Ascorbic acid for producing rGO, acting both as a reducing & protecting agent.

The crystal lattice structure of rGO obtained through the reduction of GO is similar to the pristine graphene crystal structure (Fig. 6a) with GO lattice structure containing oxygen functional groups resulting from the oxidation process (Fig. 6b). However, the reduction process of GO to yield rGO with lesser oxygen-containing functional groups often results in structural defects during the removal of functional groups (Fig. 6c).

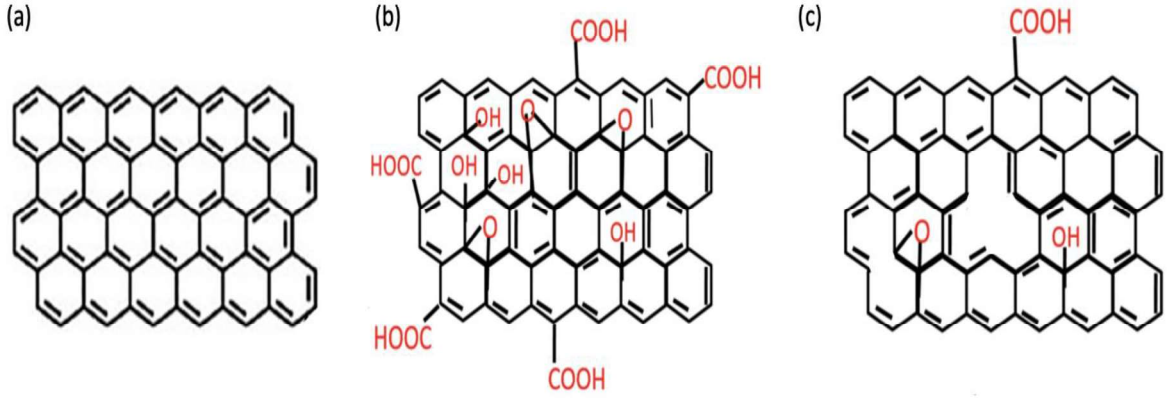

Fig. 6. The crystal lattice structure of **(a)** Pristine graphene, **(b)** Graphene oxide (GO), and **(c)** reduced graphene oxide (rGO) [98].

3.4. Hybridized Graphene

Graphene has been recently hybridized with chemical doping and combination with other materials for efficient performance in the geopolymer-based composite. Zhang et al. carried out an atomic-scale investigation of silicon-doped graphene using molecular dynamics simulations and found that the presence of silicon resulted in point defects on graphene, leading to the deterioration of its mechanical properties[99]. However, the substitutional doping of graphene with silicon enhanced the non-aggregated dispersibility of Si-graphene in aqueous solutions due to the presence of surface oxidation of silicon atoms (Si-OH) on graphene sheets, thereby promoting surface hydrophilicity and high dispersion as shown in

Fig. 7(a) and (b).

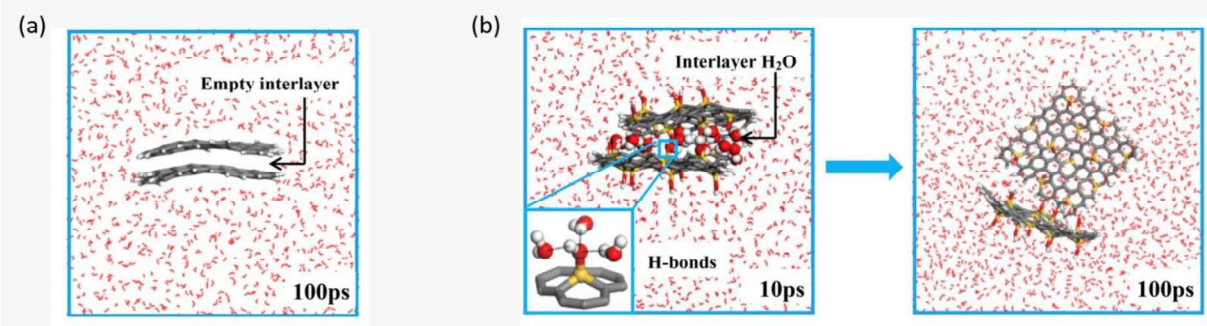

Fig. 7. (a) Dispersion mechanism of stacked graphene sheets in water with constant interlayer spacing of 0.34 nm and a potential to agglomerate, (b) Dispersion mechanism of stacked Si-graphene sheets in water with interlayer spacing up to 1.23 nm resulting from the formation of hydrogen bonds between water molecules and Si-graphene (Gray, yellow, red and white sphere represent C, Si, O, and H atoms respectively)[99].

The intercalation of titanium dioxide (TiO_2) into rGO was carried out by Guo et al. using hydrothermal synthesis to break the strong interfacial van der Waals force between layered graphene sheets[100] Results reported in their work revealed higher dispersion of prepared TiO_2-rGO nanocomposites in water when compared to rGO. The introduction of nano-TiO_2 particles from titanium dioxide [$Ti(OH)_4$] precursor onto the interlayer of rGO sheets increased the interlayer spacing, inhibiting the agglomeration of rGO sheets and promoting dispersion of TiO_2-rGO in aqueous media.

4. Graphene Reinforced Geopolymer Composites (GRGC)

4.1. GRGC Mixture Preparation

Different mix preparation process is used for producing different phases of graphene reinforced geopolymer composites, i.e., ink, paste, and aggregate-based. The key factor in mix preparation is to insure the uniform dispersion of graphene with the geopolymer matrix.

4.1.1 Ink Based

A limited number of investigations have been performed to study the behaviour of graphene geopolymer ink phases associated with its production approaches through additive manufacturing with the help of 3D printing. The rheology of the ink has a certain impact on the applicability of the manufactured products through extrusion-based 3D printing. An experimental investigation by Zhong et al. [28] revealed remarkable rheological property improvements of the geopolymer ink through the induction of GO as in Fig. 8(a). They developed the GO/geopolymer (GRGC) mixture-based ink through a typical geopolymer synthesis process (i.e., a mixture of NaOH & Na_2SiO_3 and aluminosilicates particles (ASOPs) dissolved in distilled water), which was stirred for about 20 mins, followed by GO injection into the ASOPs suspensions (< 5˚C). Another study by the same set of authors investigated the effects of GO size (i.e., large graphene oxide (LGO) & small graphene oxide (SGO)) on the reinforcement of reactive matrix (i.e., ink); SGO enhancing the mechanical properties whereas, LGO improving the rheological behaviour [47]. The GRGC ink was prepared through mechanically mixing of the GO and Sodium silicate powder (1000 revolution/min, 20 min), along with an orderly addition of sodium hydroxide and metakaolin powders followed by mechanical agitation progress (15 mins), while retaining the mass ratios GO suspensions: Sodium silicate: Metakaolin: Sodium hydroxide as 1: 0.5: 0.68: 0.075. The authors have preferred the use of sodium silicate powders over the liquid sodium silicate for obtaining a higher solid content for the GRGC ink indicated in Fig. 8(b). More efforts are necessary to determine the effectiveness of the composed ink samples to formulate optimal results.

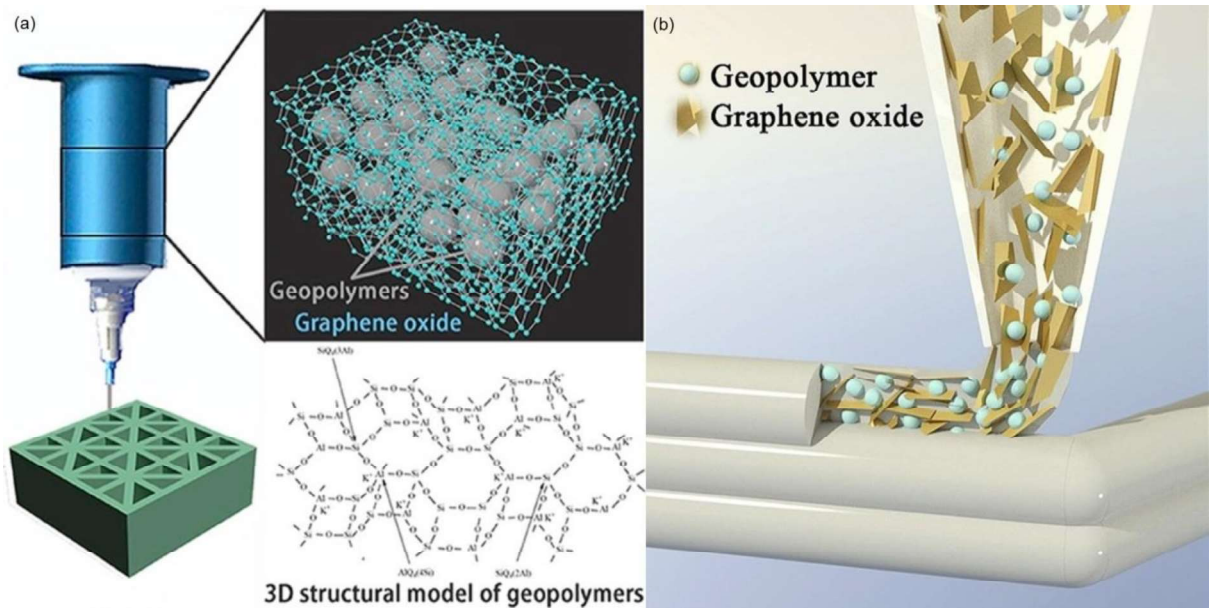

Fig. 8. (a) Illustration of the 3D printing process of GRGC, (b) Schematic diagram of 3D printing GRGC [28,47].

4.1.2 Paste Based

Relative applications provide brief distinction; separating the geopolymer paste phase from the ink phase. The researchers have adopted different methodologies for the preparation of graphene geopolymer pastes. Zhang and Lu have used a mixture of Sodium Hydroxide (NaOH) and Sodium Silicate (Na_2SiO_3) as the alkali excitant which was slowly added into metakaolin (i.e. geopolymer binder) along with the required water content [101]. The geopolymer paste was mixed slowly (2 mins) to allow even distribution of graphene dispersants as the uniformity of the dispersions in the paste plays a significant role in improving the characteristics of the resulting paste composite. Owing to the high tendency of GO and rGO to agglomerate, graphene nanoplatelets (GNP) were utilized by Candamano et al. [26] to prepare graphene geopolymer pastes. The alkali activator solution was prepared through a standard combination of NaOH and Na_2SiO_3 to which GNPs in low quantities (0.1-1% wt.) was later added followed by mechanical stirring (50 min) and sonication (210 min). Metakaolin powders were subsequently added to the solution to obtain graphene geopolymer

pastes which were further introduced to mechanical stirring and mixing (10 min). Another author, Long et al. [102] examined the effect of rGO nanosheets with varying reduction degrees on the properties of the developed geopolymer matrix. The pastes were prepared with Ground granulated blast furnace slag (GGBFS) as a binder and alkaline activators including NaOH and Na_2SiO_3 along with the in-situ reduction of GO solution through different reduction temperatures as depicted in Fig. 10. NaOH solution was instrumental in the reduction of GO solution while the rGO to slag ratio was maintained at 0.003. The pastes were further mixed at low and high speeds to produce a more stable and heterogeneous mixture. Geopolymer paste-based composite phases present a diversified preparation methodology that has been analyzed by different researchers over the years with encouraging final results. The reinforcement of graphene derivatives has been practiced at intermediate levels to sustain the toughening mechanism of the end geopolymers. Yan et al. [32] developed the geopolymer composites as indicated in Fig. 9(a), through in-situ reduction of GO by ultrasonically dispersed in water (16.67 mg/ml) for 6 hours then mixing with 0.1 M KOH and silica mixed geopolymeric solution stirring for 15 minutes and curing at 60˚C for 0.25-72 hours. In the next step, metakaolin powders were added to the rGO dispersed geopolymeric solution accompanied by ultrasonic and mechanical stir mixing for 45 minutes to produce a slurry which was cured at 60˚C for 7 days to form GRGC.

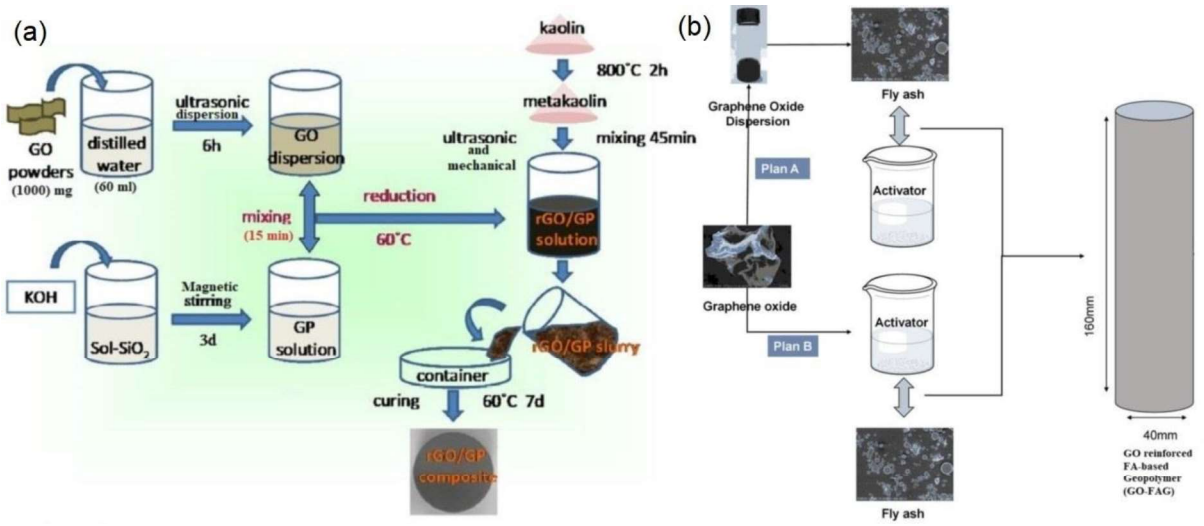

Fig. 9. (a) Schematic illustration of preparation procedure for rGO - geopolymer composite, (b) GO-FA based geopolymer matrix samples [32,84].

One of the popular methods for GRGC composite production is the dispersion of GO in water using ultrasonication then adding with alkali activator solution and mixing with alumino-silicate based geopolymer precursor. GO is hydrophilic and highly dispersible in water and ultrasonic dispersion of GO provides a rapid, efficient, and cost-effective method for procuring a homogenized GO dispersed liquid solution. The GO dispersed water is typically blended with the alkali activator solution to initiate the in-situ reduction of GO into rGO and acquire rGO based alkaline solution. In the end, alumino-silicate precursors such as metakaolin, fly ash powders are progressively added to retrieve the rGO based geopolymer slurry. Zhang et al. in their study utilized NaOH as the sole alkaline activator along with GGBFS and graphene in the ratio (GGBFS: Graphene: NaOH: Water = 1:0.0001:0.03:0.28) to produce GRGC [37]. The preliminary activities included the dispersal of graphene in water by ultrasonication and blending the mixture for 2-3 mins, and ultimately curing at 20°C (90% RH) for 1 day [37]. An advanced approach was devised by Liu et al. [84] to prepare fly ash (FA) based GRGC; demonstrating effective dispersion efficiency. In their study, GO was initially dispersed in evaporable alcohol, premixed with FA, dried into a powder, and later

mixed with Na_2SiO_3 solution which was stirred for 3 min. For the prepared GRGC samples, curing was carried out at room temperature for 24 hrs. Fig. 9(b) offers further insights into the preparation procedure of the composites.

4.1.3 Aggregate Based

Graphene geopolymer aggregate-based mortar phase is composed of a more heterogeneous system compared to ink and paste phases. Xu et al. [103] prepared the GO-influenced mortar samples as per ASTM C270 and C780 standards. The mortar samples contained sand, admixtures, activators (Na_2SiO_3, CaO, $CaCl_2$), GO, and required water content with b/s (binder/sand) ratio at 1:2 (wt.) which was mixed at room temperature for few minutes. Furthermore, Amri et al. [104] developed Palm Oil Fuel Ash (POFA) based mortar geopolymers using KOH and Na_2SiO_3 based alkaline activator solution. Graphene nanosheets (≥3 layers graphene) were added 0.1-0.7 wt% to the alkali activator solution along with POFA and sonicated for 1 hour then the solution was gradually added to sand at a POFA to a ratio of 1:3 and blended to produce a homogeneous and workable mixture. Additionally, Long et al. mixed 0.3 wt% (of slag) in-situ reduced rGO using a rotation speed up to 125±10 rpm to formulate GGBFS based geopolymer mortars with a sand-to-slag ratio of 3.0 [102]. Fig. 10, demonstrates the developmental approach for producing graphene-based geopolymer mortars and pastes. It could be noted that GO solution was mixed with NaOH solution in-situ for 3 h to produce rGO solution for the next steps of graphene reinforced geopolymer paste and mortar production. Graphene geopolymer aggregate-based concrete phases have not yet been thoroughly investigated due to the complex variations in the resulting properties. A study by Bellum et al. [8] highlighted the inclusion of GO (3 wt.%) in FA-GGBS based geopolymer concrete consisting of typical alkaline activators (Na_2SiO_3, NaOH-8M) and aggregates (crushed granite stone & river sand), followed by ambient curing conditions attained improved compressive strength (38.51 %), modulus of elasticity (28 %) and chloride

ion permeability (65.44 %).

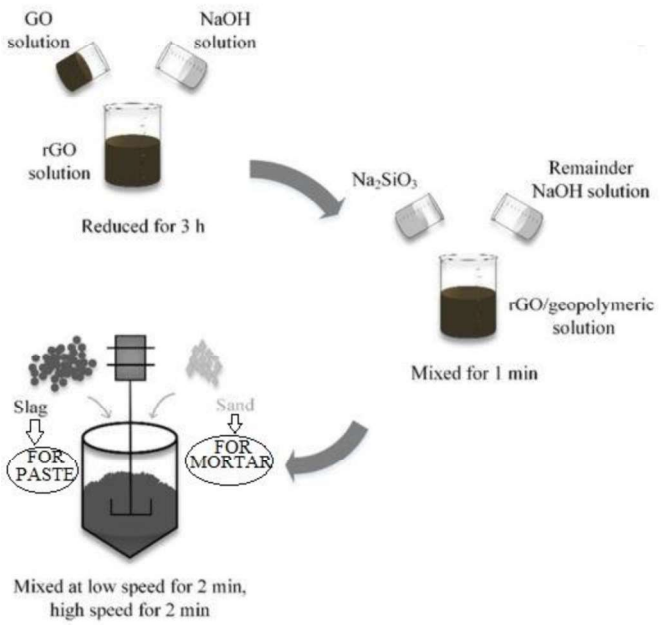

Fig. 10. Mixing procedure of rGO–geopolymer pastes and mortars [102].

4.2. Mechanical Properties

Several investigations have been conducted to determine the impact of graphene materials on the mechanical properties of GRGC. Table 4 showcases the enhancement of mechanical properties obtained through the integration of graphene nanoparticles in geopolymer composites. Several studies on cementitious materials associated with graphene reinforcement have emphasized the use of low content graphene nano additives/fillers (i.e., 0.0001-0.2 wt.%) in the GRGC for achieving superior results [37,103]. About 0.2 wt% GO reportedly increases 23.21% compressive strength of GRGC mortar compared to the plain geopolymer mortar [103]. Consequently, higher content graphene nano additives/fillers (i.e., ≥1 wt.%) have also been investigated by different researchers [28,101]. Ranjbar et al. [19] reported an increase in flexural strength, flexural toughness, and compressive strength by 216%, 300%, 144% respectively with the addition of GNP (1% wt.) in the geopolymer composites. The toughening mechanism of the GNP in the geopolymer matrix can be

certainly interpreted through the detailed schematics in Fig 11(a) & (b); wherein the GRGC composite specimens are subjected to flexural and compressive load. The GNP can serve as 2D nano-reinforcing sheets enhancing the crack deflection and obstructing crack propagation under uniform and non-uniform stress.

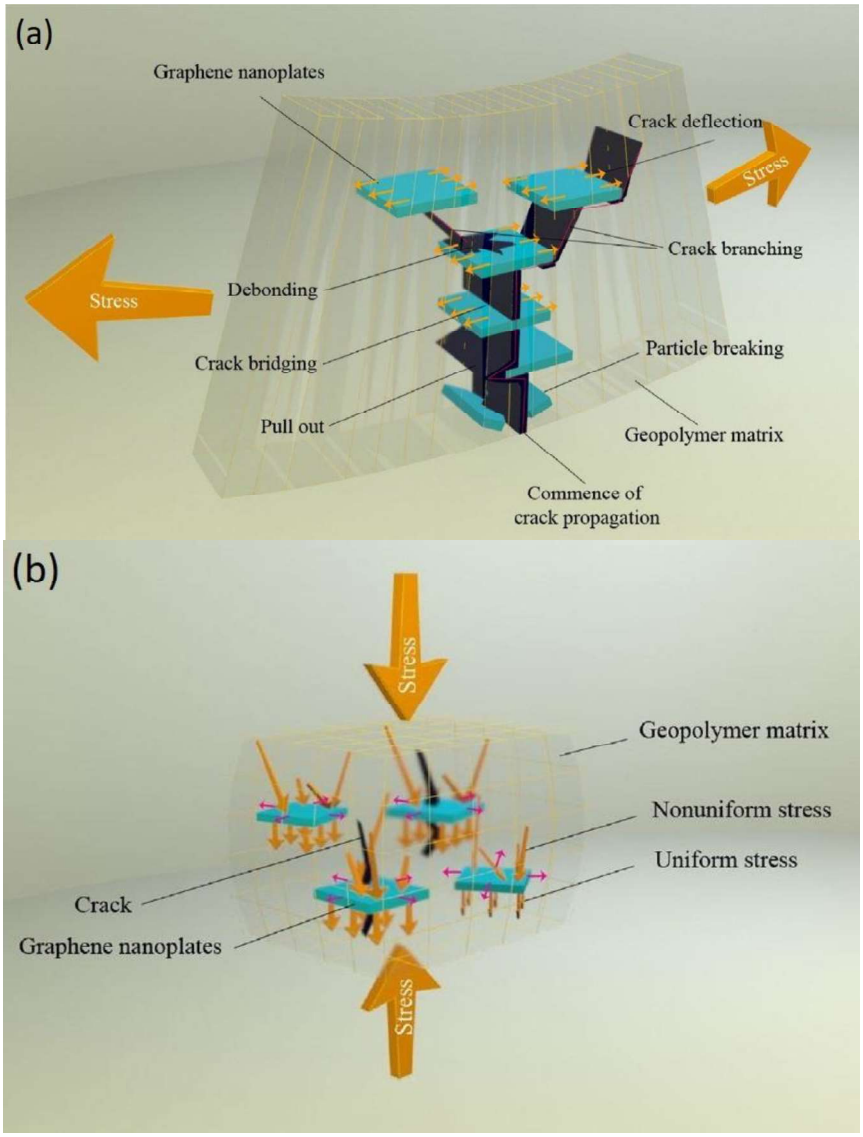

Fig. 11. Illustration of a GNP-FA geopolymer composite (a) under a flexural load, (b) under a compression load [19].

The mechanical properties of the GRGC are adequately correlated with the dispersion of graphene in the geopolymer matrix. Certain studies have stated the negative impacts

associated with a higher amount of graphene additives (GA) (i.e., <3 wt.%) such as uneven dispersion and susceptibility to agglomerate which eventually deteriorates the mechanical strength of the composites [101]. Agglomeration decreases the bonding between geopolymer and GA and increases the porosity as well as the formation of fracture origins in GRGC. The integration threshold for GA is critical and is determined by its geopolymer binder type, form, and mix nature. A cut-off limit of 0.5 wt.% with rGO-GA and 0.3 wt.% with GO-GA have been observed for FA-based geopolymer matrix [31,84], whereas, the authors have not come across any investigation highlighting the use of pristine graphene additives from the relevant literature studies.

GO, and rGO have both been instrumental in refining the geopolymer matrix at very low loadings to obtain the maximum attainable mechanical properties for the geopolymer composites. Xu et al. [103] have outlined the functionality of GO in enhancing the compressive strength of an FA-based geopolymer matrix by 23% with the addition of 0.02% GO by the mass of FA [103]. GO ameliorated the polymerization degree of FA-based geopolymer matrix while modulating the (Si/Al, Ca/Si, Ca/(Si+Al)) mole ratios to promote the development of FA hydrates (i.e., quartz, jennite) resulting in increased rigidity and toughness. The improved toughness was elaborated by Ranjbar et al. as GO tends to absorb the energy when exposed to crack-bridging or pull-out [19]. According to Liu et al. [84], GO promotes geopolymer hydration by strong reactive electrons and functional groups containing oxygen and performs a pivotal contribution in the development of the mechanical strength of GRGC. The substantial surface area and high van der Waal's force of GO hinder its ability to uniformly disperse in geopolymer paste, while the non-uniform distribution of GO concludes in inadequate mechanical strength resulting from the dissemination of microcracks [105,106]. The encapsulation effect of GO further inhibits the enhancement of mechanical properties. On the other hand, rGO possesses fewer residual oxygen-containing functional groups that

support its uniform dispersion as a result of electrostatic stabilization in the alkaline environment of the geopolymer matrix [107]. An alternative investigation by Zhang et al. introduced GNP (1 wt. %) as an electron acceptor in an FA-based geopolymer matrix to enhance its electroconductivity up to about 348.8% [35]. Moreover, Yan et al. [107] credited the strength enhancement of rGO-GP towards the firm interface bonding among rGO and the geopolymer matrix with rGO pulling-out, wrapping, and anchoring themselves around geopolymeric particles and playing a leading part in enhancing the GRGC's strength to transmit load effectively. The rGO's wrinkled surface leads to the strong bonding condition in rGO-GP, and this effective interfacial attachment can be interpreted by mechanical interlocking combined with chemical cross-linking form bonding, which further increases the compressive strength as rGO dissipates the stress effectively [108].

Ultimately, due to different functional groups such as epoxy, hydroxyl, carbonyl, and carboxyl groups along with dispersion efficiencies, GO, and rGO demonstrate distinct effectiveness in enhancing the hydration degree and mechanical behaviour of geopolymer composite matrix. Geopolymer materials crystallize on exposure to heat treatment which sequentially enhances the mechanical properties [108]. Yan et al. [109] observed a 471% rise in flexural strength and a 775% rise in fracture toughness of rGO based GRGC compared to the geopolymer without rGO while exposed to 950°C for 0.5 hr. However, the properties deteriorated with further exposure to increased temperature.

4.3 Electrical Properties

The electrical properties of GRGC have been explored by different researchers. Saafi et al. [30] enhanced the electrical conductivity of an FA-based geopolymer matrix (0.77 S m^{-1}) by 209.09% through the inclusion of 0.35 wt.% rGO. The successful development of conductive networks from the electrolytic conductors (i.e., conductive pores) found in the FA-based

geopolymer matrix is amplified by rGO; thereby facilitating the GRGC to carry high current densities with improved gauge factors. The authors also investigated the piezoresistive effects of the GRGC in which the relative resistance variation ($\Delta R/R_0$) rises linearly with increasing tensile strain and reduces linearly with increasing compressive strain. An alternative investigation by Zhang et al. [35] introduced GNP (1 wt.%) as an electron acceptor in an FA-GPC to enhance its electroconductivity up to about 348.8%. The electrochemical impedance spectroscopy (EIS) study confirmed the improvement as the GRGC exhibited smaller electrochemical impedance with regard to FA-based geopolymer matrix, implying weaker resistance intensity in the solid-state interface layers and more effective transfers of interfacial charges. The synergistic effect of GNP and FA-based geopolymer matrix provides scope for extending the spectral response of GRGC to longer wavelength ranges. Composites incorporating GO are electrically insulating due to the non-conductive nature of GO for the presence of oxygen-containing functional groups as defects in graphene surfaces [110]. Hence, GO should not be used as a conductive filler. Various reduction methods are carried out to regain the electrical conductivity of GO. Thermal annealing and chemical reduction methods are widely used to reduce the functional groups in GO and produce different grades of rGO with electric conductive properties [30].

The agglomerated stacks can be considered as 'conductive islands' in comparison to the detrimental effects of GA agglomeration on mechanical properties, contributing to establish percolation networks within the matrix [111]. Related phenomena have been observed in several GRGC specimens. Likewise, Zhong et al. [28] achieved an electrical conductivity of 10^2 S m^{-1}; considered to be very high among ceramic nanocomposites; through thermal annealing of GO-GPC, resulting in a high electrically conductive network. Xu and Zhang (2017) have developed a structural supercapacitor with a peak specific capacitance of 36.5 Fg^{-1} with dual graphene electrodes sandwiched with one geopolymer separator and saturated

with 2 M KOH electrolytes [48]. The authors noted a correlation between the geopolymer activator solution modulus and the curing age with the capacitance value as the geopolymer's internal resistance rises as the modulus decreases and the curing age expands due to the decrease in porosity and vice versa. Incongruous changes in electrical and mechanical properties brought by the introduction of GA for the production of GRGC, in particular those intended for structural application, should be considered.

Table 4. Property enhancements of geopolymers attributed to the reinforcement of graphene.

Ref.	Specimen Type	Geopolymer Precursors and Activators	Graphene Reinforcement Type	Graphene Dosage	Curing Graphene Reinforcement Type Conditions	Mechanical Performance Increase (%)	Highlights
Saafi et al. 2015 [31]	Paste based GRGC	Fly Ash (F) + (Na_2SiO_3 + 10 M NaOH)	rGO sheets	0.50 wt.%	25 °C (2 hr.) + 60 °C (24 hr.)	Young Modulus: 376% Flexural Strength: 134% Flexural Toughness: 48%	rGO sheets at minimal quantities advance the mechanical behavior and reduce the overall porosity of geopolymer.
Ranjbar et al. 2015 [19]	Paste based GRGC	Fly Ash (F) + (Na_2SiO_3 + 16 M NaOH)	GNP's	1 wt.%	Ambient Conditions (1 hr.) + 65 °C (24 hr.)	Flexural Strength: 216% Flexural Toughness: 300% Compressive Strength: 144%	Low filler weight proportions of GNP fillers are competent enough to enhance the toughness, stress, and strain at the initial crack along with the rigidity of geopolymer.
Yan et al. 2015 [32]	Paste based GRGC	Metakaolin + (KOH + Silica Soln.)	GO/rGO	1 wt.%	60 °C (7 Days)	Flexural Strength: 5% Fracture Toughness: 17%	In situ reduction of GO in alkaline geopolymeric solution resulted in a strong interfacial bonded geopolymer matrix with enhanced mechanical properties.
Yan et al. 2016 [109]	Paste based GRGC	Metakaolin + (KOH + Silica Soln.)	rGO	1 wt.%	60 °C (7 Days) + 950◦C (0.5 hr.)	Flexural Strength: 470% Fracture Toughness: 775%	Mechanical properties of rGO-GP are positively influenced by isothermal soaking resulting in a low onset temperature (~1000◦C) of crystallization.
Yan et al. 2016 [107]	Paste based GRGC	Metakaolin + (KOH + Silica Soln.)	GO/rGO	0.3*/0.5** wt.%	60 °C (7 Days)	Flexural Strength: 45%* Fracture Toughness: 61.5%**	Improved interface connection between the rGO and the geopolymer matrix contributed to crack deflection and spread owing to rGO pulling out, wrapping, and stabilizing around geopolymeric particles.
Yan et al. 2016 [112]	Paste based GRGC	Metakaolin + (KOH + Silica Soln.)	GO/rGO	1 wt.%	60 °C (7 Days) + 1000°C (0.5 hr.)	Elastic Modulus: 8% Flexural Strength: 120% Fracture Toughness: 1.5% Vickers hardness: 29%	High-temperature treatment on in situ reduced rGO/geopolymer composite has overall improvement effects on its mechanical properties.
Yan et al. 2016 [113]	Paste based GRGC	Metakaolin + (CsOH/KOH + Silica Soln.)	GO/rGO	1 wt.%	60 °C (7 Days) + 1000°C*/1100° C** (0.5 hr.)	Flexural Strength: 37%* Fracture Toughness: 20%**	Prolonged exposures to high temperatures increased the rolled and wrinkle characteristics of rGO sheets along with the refinement of cubic leucite grains.
Yan et al. 2017 [33]	Paste based GRGC	Metakaolin + (CsOH/KOH + Silica Soln.)	GO/rGO	1 wt.%	60 °C + 24 hr.	Flexural Strength: 7% Fracture Toughness: 30%	Addition of GO in geopolymer matrix expedited the transformation of Al–O sites into four coordinates and Si atoms in the form of $Q_4(3Al)$, while the matrix attached properly with the rGO sheets and exhibited denser microstructure
Zhong et al. 2017 [28]	Ink based GRGC	ASOPs + ALSPs	GO	5 wt.%	17 °C (5 Days) + 1000°C (0.5 hr.)	Elastic Modulus: 43% Compressive Strength: 50%	The rheology of geopolymer precursors is greatly influenced by the inclusion of GO; thereby facilitating the 3D printing of geopolymer and indicating a strong GO-HGPP engagement.
Zhang et al. 2018 [35]	Paste based GRGC	Fly Ash + (Na_2SiO_3 + KOH)	GNP	1 wt.%	80 ◦C (6 hr.) + Ambient Condition (18 hr.)	Electroconductivity: 348.8%	The spectral response of GR/FAG composite can be stretched to a broader wavelength range with an increased graphene composition attributed to the synergistic effect of GNP and Fly ash Geopolymer.
Zhang	Paste	Metakaolin +	Graphene	3 wt.%	20 °C (3 Days	Compressive Strength: 287%	Graphene's influence in enhancing the strength of the geopolymer is

and Lu, 2018 [101]	based GRGC	(Na_2SiO_3 + NaOH)					gradually weakened beyond a certain degree.
Candamano et al. 2019 [26]	Paste based GRGC	Metakaolin + (Na_2SiO_3 + NaOH)	GNP	0.5 wt.%	50°C (24 hr.)	Young Modulus: 14.66% Tensile Strength: 14.44%	GNP/geopolymer composites show electro-mechanical behavior with a charge coefficient of 11.99 pC/N and increased stiffness and strength.
Xu et al. 2018 [103]	Aggregate based GRGC	Fly Ash + (Na_2SiO_3 + CaO + $CaCl_2$)	GO	0.02 wt.%	Ambient Conditions (28 Days)	Compressive Strength: 23.21%	The polymerization level of the FA-geopolymer has been elevated by GO, as the total silica in the form of Q3 and Q4 also rises.
Zhang et al. 2018 [36]	Paste based GRGC	Granulated Blast Furnace Slag + NaOH	Graphene	0.02 wt.%	20°C (28 Days)	Flexural Strength: 96.2% Compressive Strength: 31.10%	GRSN composite was utilized as a photocatalyst for solar green hydrogen production with increased efficiency through graphene inclusion.
Amri et al. 2019 [104]	Aggregate based GRGC	POFA + (Na_2SiO_3 + 10 M KOH)	GN	0.7 wt.%	60 °C (24 hr.) + Ambient Conditions (28 Days)	Compressive Strength: 74.19 %	SEM micrographs implied that graphene-enhanced surface morphology by decreasing the porosity of geopolymers with a pore-filling system due to the very small particle size of graphene.
Long et al. 2019 [102]	Paste & Aggregate based GRGC	GGBFS + (Na_2SiO_3 + NaOH)	GO/rGO	0.003 wt.%	60 °C (24 hr.) + 80 °C (48 hr.)	Flexural Strength: 51.2%	Hydration of specimens dramatically increases as rGO nanosheets increase the relative concentration of OH= ions and offer additional nucleation sites for the development of C-S-H and C-A-S-H gels.
Zhang et al. 2020 [37]	Paste based GRGC	GGBFS + NaOH	Graphene	0.0001 wt.%	20 °C (24 hr.) + Ambient Conditions (28 Days)	Flexural Strength: 96.15% Compressive Strength: 31.02%	ZnO-loaded GASG nanocomposites with excellent photocatalytic activity lead to the generation of hydrogen and the disintegration of dye wastewater, which has been due to the synergistic effect of ZnO semiconductor, graphene, and ASG.
Liu et al. 2020 [84]	Paste based GRGC	Fly Ash (F) + (Na_2SiO_3 + NaOH)	GO*/rGO**	0.30[a]/0.10[b] wt.%	Ambient Conditions (24 hr.) + 25 °C (28 Days)	Flexural Strength: 25%*[a]/10%**[b]	GO/rGO decreases the porosity of geopolymers by stimulating the development of geopolymer gel and packing of nanoscale pores with self-adsorbed zeolites and other materials.
Long et al. 2020 [114]	Paste based GRGC	(GGBFS + SF + EPS beads) + (Na_2SiO_3 + NaOH)	GO/rGO	0.04 wt.%	20 °C (24 hr.) + 20 °C (28 Days)	Flexural Strength: 26.5% Compressive Strength: 29.8%	rGO-WEA can accelerate the recycling of EPS wastes and to facilitate sustainable structural and efficient cementitious composites for the building industry.
Saafi et al. 2014 [30]	Paste based GRGC	Fly Ash + (Na_2SiO_3 + NaOH)	GO/rGO	0.35wt.%	25 °C (2 hr.) + 60 °C (24 hr.)	Electroconductivity: 209.09 %	The addition of rGO in geopolymeric composites showed a quite sensitive and linear reactions to axial tensile and compressive strain which suggested prospective use as self-sensing building components.

4.4 Microstructure

The GRGC microstructure is extensively investigated using X-ray diffraction (XRD), Fourier-transform infrared spectroscopy (FTIR), Thermogravimetric analysis (TGA), and various electronic microscopic imaging observations such as Scanning Electron Microscope (SEM) and Energy dispersive X-ray (EDX) elemental quantification. An extensive review of the characterization instruments utilized in the field of GRGC has been detailed in table 5. The microstructural observation is carried out to study the physicochemical interplay between the 2D graphene planes and the geopolymer matrix, which clarifies the alteration of the GRGC properties. This section describes the advancement of the understanding of the GRGC microstructure.

4.4.1 XRD Analysis

The XRD patterns of FA-based geopolymer matrix imply the presence of quartz, mullite, and albite as typical crystalline phases. A series of studies suggest that the integration of graphene materials on the geopolymer-based composite has not contributed to the formation of any new additional compounds in the geopolymer matrix [19,33,107,109]. This may be attributable to the low fraction of volume (<5 percent) and nano size of graphene materials that can be explicitly be detected by XRD [109]. The XRD analysis of the FA-based geopolymer reinforced with 1 wt.% of a particular GNP, by researchers indicates no difference in XRD patterns for GNP [19]. Both geopolymers with and without GNP are composed of common crystalline phases of quartz and mullite (developing from FA) and a scarce amount of albite [26]. A pure geopolymer and an rGO-geopolymer composite with 1 wt.% rGO display broad amorphous humps around 28° 2θ in XRD which stated that rGO might have a slight impact on the microstructure of the composite [32,115]. The XRD patterns of rGO-geopolymer composite with different dosages of rGO were analyzed in

another study conducted by the same authors [115] as presented in Fig. 12. A broad amorphous hump at 28° with no phase structural shift of rGO-geopolymer samples can be observed as discussed above.

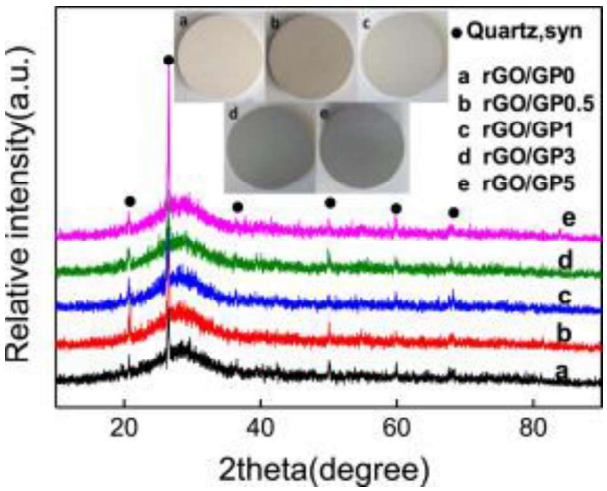

Fig. 12. XRD curves of rGO-geopolymer composites with different dosage in percent of geopolymer: (a) 0 wt.% rGO, (b) 0.5 wt.% rGO, (c) 1 wt.% rGO, (d) 3 wt.% rGO and **(e)** 5 wt.% rGO [115].

Graphene materials are reported to influence the development of amorphous phases in the Portland cement (PC) hydration process by other groups of researchers [108,116,117]. Various peaks in the rGO-geopolymer composites were observed and identified as α-quartz. Distinctive rGO peaks were not detected by XRD analysis but were noticed by Raman Spectroscopy. Usual geopolymer broad humps around 17–32° at 2θ were identified from the XRD pattern along with a slight α-quartz phase [33]. Zhou et al. [47] suggest that both fresh geopolymer and GO reinforced geopolymer composites exhibit similar non-crystallinity, yet different diffraction peaks for different sizes of GO planes. Therefore, different size, surface chemistry of GO could cause some change to GRGC. The TGA is sometimes reported to be more appropriate to determine the crystallization temperature for geopolymer compared to

XRD [109]. Although the leucite turns into a significant phase upon heating the geopolymer-based composite, rGO fails to inherently influence the leucite crystallization temperature.

4.4.2 FTIR Analysis

The FTIR spectra analysis is useful for understanding the impact of graphene materials on geopolymer-based composite microstructural interaction. A group of researchers suggests that normal geopolymer and GRGC show similar major FTIR bands [19]. The intensity band at 445 cm^{-1} was accredited to Si-O-Si bending vibration, and the band at 990 cm^{-1} was detected because of Si–O–Al asymmetric stretching vibration. Furthermore, the band near 780 cm^{-1} is associated with quartz in its crystalline phase. O-H bending was assigned to the band at 1650 cm^{-1}. Asymmetric and symmetric stretching of methylene groups (CH_2) is recognized from the bands located at 2920 $cm^{-1}$and 2840 cm^{-1}, respectively. The FTIR spectra remain mostly unchanged for both samples; with and without rGO. The bands at 463 cm^{-1}, 593 cm^{-1}, and 717 cm^{-1} suggested the creation of a large number of Si–O–Si, Si–O–Al, and AlO_4 configuration units in the reaction products. In another study, the rGO geopolymer composites revealed higher organic content at ~1500 cm^{-1} in contrast to that of 100% geopolymers [31]. The GO in the geopolymers may have been reduced during the processing when the high depreciation of the hydroxyl and carbonyl groups implies the diminution of GO's functional groups through deoxygenation by alkali NaOH [118,119]. Even a low concentration of NaOH solution results in the aggregation of GO due to their deoxygenation reaction with NaOH; this can be visually noted in Fig. 13(a). As a function of excitation and emission wavelengths, the fluorescence intensity is displayed in color in Fig. 13(b) & (c). GO after dispersion in water shows a single broad emission centered around an excitation wavelength of 425 nm (Fig. 13(b)). In contrast, GO dispersion in NaOH solution is strongly wavelength-dependent. This chemical interaction is also indicated in FTIR (Fig. 14) when the chemical reduction of hydroxyl and carbonyl functional groups related peaks reduced and C-

H peaks at ~1500 cm^{-1} mostly remain intact [31]. Besides the Si-O covalent bond absorbance amplification is possibly due to the cross-linking within the rGO planes and FA matrix. Other similar studies suggest that GO undergoes in situ reductions when geopolymer is treated activated in a high alkaline environment [107,115]. The in-situ reductions of GO to rGO within geopolymer composite FTIR spectra show a dramatic decrease of the characteristic bands in the oxygen functional groups, specifically, the C=O peak at 1720 cm^{-1} is dramatically diminished. The size of GO was also reported to have some influence on the GO-geopolymer composite FTIR absorption peak. The long plane size of GO in the geopolymer composite considerably exhibits a high absorption peak equivalent to free water at 3467 cm^{-1}, and 1653 cm^{-1} compared to short plane GO [47]. Also, the tetrahedral structure of SiO_4 results in a peak at wavenumber 992 cm^{-1} for long plane GO in the geopolymer, while the peak is relocated to 977 cm^{-1} for short plane GO in the composite.

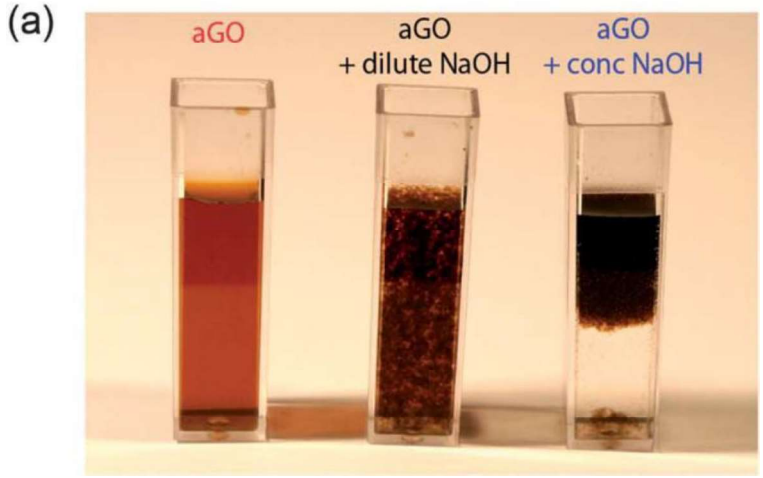

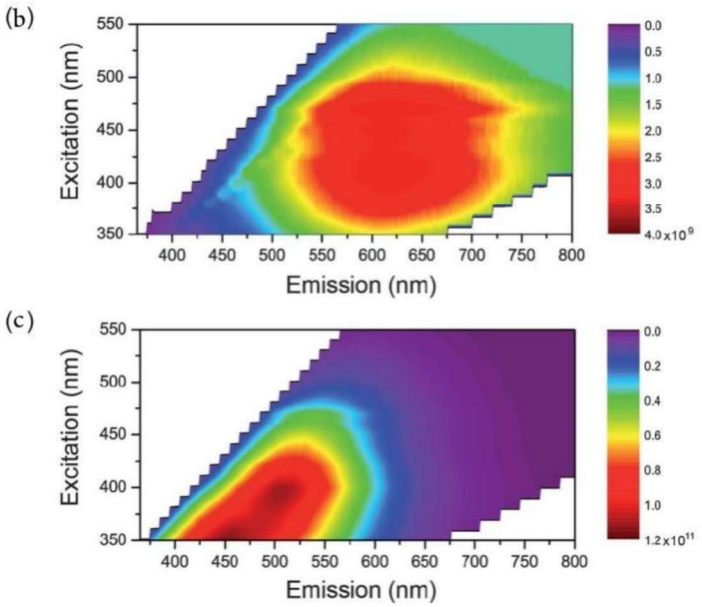

Fig. 13. Impact of highly alkaline NaOH solution on the GO aggregation: (a) photographs of GO dispersion (left) as dispersed in water 0.75 mg ml^{-1}, (center) after adding diluted NaOH, and (right) after adding concentrated NaOH, (b) fluorescence intensity map as a function of excitation and emission wavelengths as-produced GO, and (c) intensity maps of oxidation debris [119].

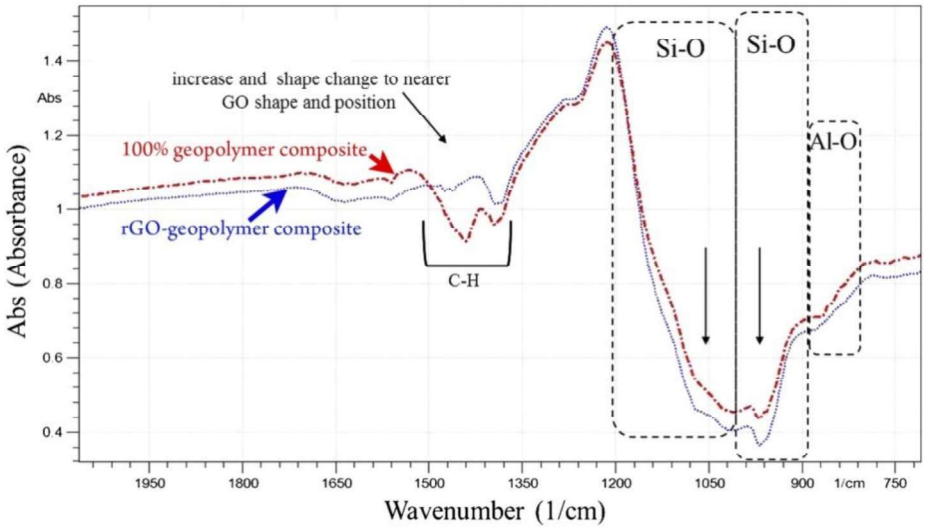

Fig. 14. Diffuse FTIR spectra of 100% geopolymer and rGO-geopolymer composites [31].

4.4.3 TEM Image Observation

The TEM images from an rGO-geopolymer composite in Fig. 15 suggest that rGO sheets having a size (width) of 5-15 μm are visible and uniformly distributed in the matrix. The geopolymer-covered rGO sheet display Deby ring with three apparent diffraction marks which could be formed due to the hexagonal shape of graphene. Within another similar study, the samples were characterized by TEM, and it was observed that there exists a good bonding state between crystal rGO and the matrix of geopolymer which comprises fine sphere particles [107]. The TEM image analysis shows clear interaction between graphene materials and the geopolymer matrix.

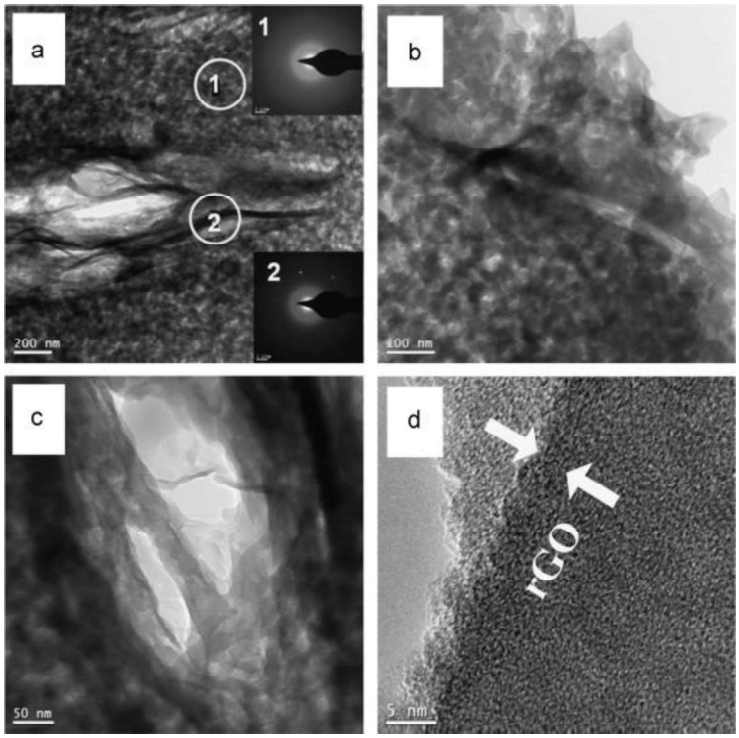

Fig. 15. TEM images of rGO-geopolymer composite: (a) wrinkled rGO sheets and SAED pattern of geopolymer composite matrix, (b) and (c) rGO sheets within fine particles off geopolymer matrix, and (d) rGO sheet enclosed with the geopolymer matrix [32].

4.4.4 SEM Image Observation

The presence of graphene materials can be detected through SEM observation. The SEM

images revealed the visibility of rGO sheets which were dispersed in a uniform manner inside the geopolymer matrix [115]. The microstructure and the density of the GRGC are improved by the rGO incorporation [31]. A characteristic feature of FA, a highly siliceous wide distribution of mostly submicron to micron range spherical particles is observed in the SEM micrograph. The rGO sheets and their clusters within the FA particles covered the voids along with the spaces in the matrix (Fig. 16). Cross-linking and functionalization upon the surface of the rGO sheets and the FA particle might have occurred, which can be seen in Fig. 16 (c and d) where FA particles are coated with thin rGO sheets, generating a "mushroom" shape. Saafi et al. [31] suggest that the exchange between rGO and FA occurs primarily through electrical induction, which causes the rGO sheets to adsorb onto the FA particles. They also suggest that "the in-situ cross-linked particles in the form of [−Si–O–]x[rGO]y[−O–Si–]z (with x ⩾ 1, y⩾ 1 and z ⩾ 0) are developed in the rGO–geopolymeric matrices".

Further according to the 29Si MAS NMR spectra study, it was established that the Al substitution on the end-of-chain silicate of C-(A)-S-H gels could be limited by the use of rGO sheets [102]. This is owing to the major structural defects in the rGO sheet formed during the alkali reduction below 80 °C, which limits the substitution of Al in the hydration compounds of geopolymers. Besides that, the long plane GO can hold a large number of geopolymer particles and form extensive surface coverage of the geopolymer composite [47]. In contrast, a short plane GO sheet trigger more open holes on the composite surface which considerably affects the water evaporation of GO-geopolymer composite during the curing process.

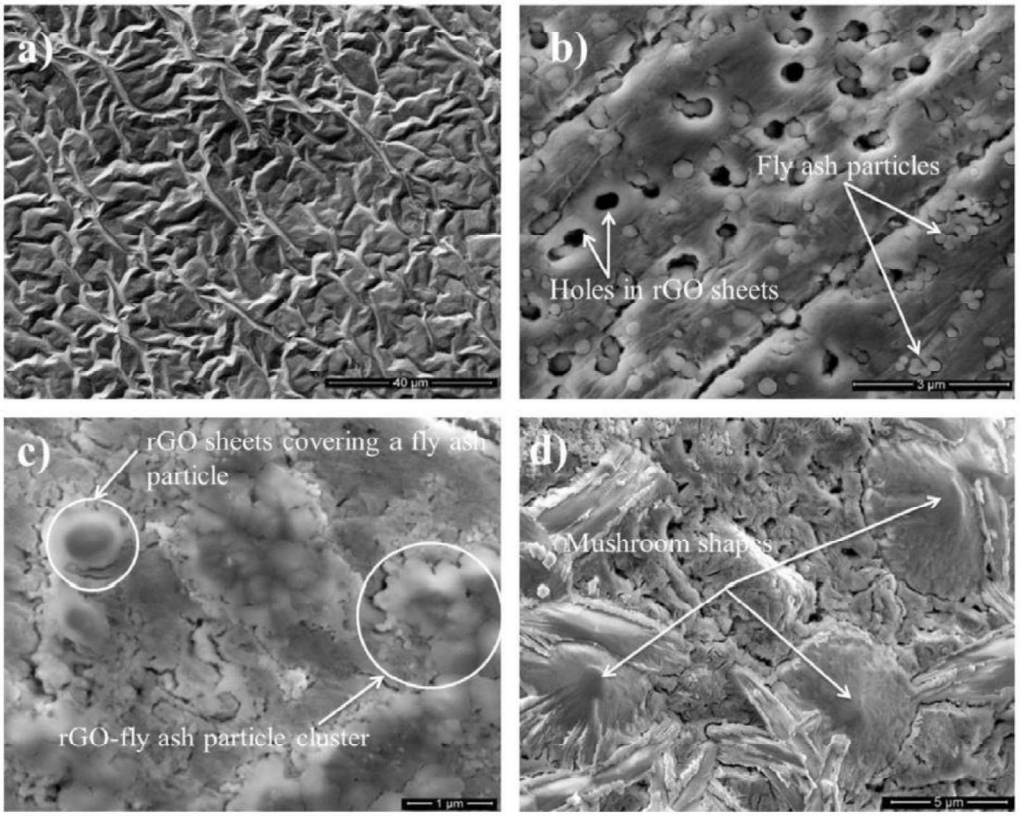

Fig. 16. SEM image of graphene geopolymer composite, (a) rGO, (b) 0.35-wt.% GO sheet interaction with submicron fly ash, (c) 0.35-wt.% GO sheets covering submicron fly ash particles and (d) 0.35-wt.% GO sheet interaction with larger fly ash particles [31].

The mechanical interaction takes place through the particle interlocking between the textured and wrinkled morphology of rGO nanoparticles and the geopolymer. The coarse texture of the GNP surface extends the area of contact between the geopolymer matrix and the GNPs, which eventually increases the energy of pull-out and debonding while improving the mechanical properties of the composite [19]. The pull-out of wrinkled rGO sheets is reported at the fracture surfaces of the rGO-geopolymer composites in different studies [109]. The number of edges projecting (sticking out) from the fracture surface of the rGO-geopolymer matrix elevated when the dosage of rGO was increased [115].

Table 5. Characterization instruments of graphene geopolymer composite.

Ref.	Specimen	Analysis Type	Instrument	Specifications
Saafi et al. 2014 [30]	Paste based GRGC	Electrical Conductivity	Keithley 6221, Extech ex 503	AC/DC (50 mA)
Saafi et al. 2015 [31]	Paste based GRGC	FTIR (Fourier Transform Infrared Spectroscopy)	4100 ExoScan	Resolution (8 cm^{-1})
Ranjbar et al. 2015 [19]	Fly ash	XRF	PANalytical AXIOS-MAX	
	Graphene Nanoplatelets	AFM (Atomic Force Microscopy)	Veeco Dimension	Tapping mode
	Paste based GRGC	BET (Brunauer–Emmett–Teller) Specific Surface Area	BELSORP-MAX	Nitrogen Adsorption Isotherms, 77K
	Paste based GRGC	TEM (Transmission Electron Microscopy)	CARL ZEISS-LIBRA 120	
	Paste based GRGC	FESEM (Field emission scan electron microscopy)	CARL ZEISS-AURIGA 60, Quanta FEG 450	
	Paste based GRGC	XRD (X-ray Diffraction)	PANalytical Empyrean	Monochromated Cu Kα radiation (λ = 1.54056 Å), 45 kV, 40 mA, Step Size=0.026°, Scanning Rate= 0.1 deg $^{s-1}$ 2θ (20-70) °
	Paste based GRGC	FTIR	Perkin Elmer System series 2000	Frequency Range (4000-400 cm^{-1})
	Paste based GRGC	Static Water-Contact Angle	OCA 15EC	
	Paste based GRGC	Compressive, Flexural Strength, Young's Modulus, Flexural toughness	INSTRON-3369	ASTM C293-10, ASTM C1018-97
	Paste based GRGC	Toughening Mechanisms	Mitutoyo AVK-C2	
Yan et al. 2015 [32]	GO (Graphene Oxide), rGO (Reduced Graphene Oxide)	FTIR	Nicolet Nexus 6700	ATR Measurement Mode
	GO, rGO	Raman spectroscopy	HORIBA Jobin Yvon HR-800	50x objective lens, 532nm laser excitation
	GO, rGO	XPS (X-ray Photoelectron Spectroscopy)	PHI 5700 ESCA System	
	GO, Paste based GRGC	SEM	FEI Quanta 200 FEG	
	GO, rGO, Paste based GRGC	TEM	TECNAI G2 FEG	200kV
	Paste based GRGC	XRD	Rigaku RINT-2000	Cu-Ka radiation
	Paste based GRGC	Flexural Strength	Instron-5569	Span Length-20 mm, Speed-0.5 mm/min
Zhang et al. 2016 [120]	Graphene, Slag, Paste based Nano GRGC	FESEM	Hitachi S-4800	
	Slag, Paste based Nano GRGC	DRS (UV-visible Diffuse Reflectance Spectrum)	HITACHI UV-4100	
	Slag, Paste based Nano GRGC	PSD (Pore Size Distribution)	Micromeritics ASAP 2020	Liquid N_2 (−196°C)
	Paste based Nano GRGC	Compressive Strength	YAW-300	Loading Speed-2.4 kN/s
Yan et al. 2016 [109]	Paste based GRGC	DTA (Differential Thermal Analysis)	Netzsch STA 449C	
	Paste based GRGC	SEM	FEI Helios NanoLab 600i	
	Paste based GRGC	Flexural Strength	Instron-5569	Span Length-20 mm, Speed-0.5 mm/min, ASTM C1161-02c
Saafi et al. 2016 [27]	Paste based GRGC (Sensor)	EIS (Electrical Impedance Spectroscopy)	Gamry Interface 1000 Potentiostat	Frequency (0.04 Hz–5 kHz),
Yan et al. 2016 [112]	Paste based GRGC	Raman spectroscopy	Renishaw In Via	532 nm Laser
	Paste based GRGC, Leucite	XRD	PANalytical X'Pert PRO	CuKα (k = 1.5406 nm), Continuous scan mode
	Paste based GRGC	TEM	FEI Tecnai G2 F30	
	Paste based GRGC	DTA, TG (Thermal gravimetric analysis)	Netzsch STA 449C	

	Paste based GRGC	TS (Thermal Shrinkage)	Netzsch DIL 402C	5°C/min/Ar
	Paste based GRGC	Flexural Strength	Instron-5569	Span Length-20 mm, Speed-0.5 mm/min
Zhong et al. 2017 [28]	Ink-Paste based GRGC	Rheology	Discovery Hybrid Rheometer HR-1	Room Temperature
	Ink-Paste based GRGC (3D Printed)	Mechanical Properties	UTM (Universal Testing Machine) AG-IS	Compression Speed (0.5 mm s^{-1})
	Ink-Paste based GRGC (3D Printed)	FTIR	Agilent Cary 660	
Zhang et al. 2017 [34]	Paste based GRGC	XRF	Bruker S4 Pioneer	
	Source Materials, Paste based GRGC	XRD	Rigaku D/MAX2200	CuKα radiation, 40 mA, 40 kV
	Paste based GRGC	TG, DTG (Differential Thermogravimetry), DSC (Differential Scanning Calorimetry)	Mettler Toledo TGA/DSC1	Inert Nitrogen Atmosphere
	Paste based GRGC	BET Specific Surface Area	ASAP 2020	Liquid N_2 (77K)
	Paste based GRGC	PL (Photoluminescence Spectroscopy)	Hitachi F-4500	150w Xenon Lamp, 425 nm
	Paste based GRGC	XPS	AXIS SUPRA	Al Kα (1486.6eV)
Yan et al. 2017 [33]	Paste based GRGC	SEM	Helios NanoLab 600i	
	Paste based GRGC	NMR (Nuclear Magnetic Resonance)	Bruker Avance III 400	Magnetic Field Strength (9.4 T), 4 mm rotor
Zhang et al. 2018 [35]	Paste based GRGC	Electroconductivity	ITECH (IT6833, 72V, 3A), UNI-T (UT39A)	
	Paste based GRGC	PL	Hitachi F-4500	428 nm
	Paste based GRGC	XPS	AXIS SUPRA	Monochromatic Al Kα anode, 15 kV, 8 mA
	Paste based GRGC	Nitrogen Adsorption/Desorption Isotherms	Micromeritics ASAP 2020	Liquid N_2= -192°C
	Paste based GRGC	Raman spectroscopy	Horiba LabRAM HR Evolution	785 nm laser diode, 290 mW
	Paste based GRGC	EIS	CHI 660E	
Xu et al. 2018 [103]	Aggregate based GRGC	EPMA/WDS (electron probe microanalysis/wavelength dispersive X-ray spectroscopy)	JEOL JXA-8500F	15 kV, 50 nA
Zhang et al. 2018 [36]	Paste based Nano GRGC	Flexural strength	DKZ- 5000	Loading Speed (50 N/s)
	Slag, Paste based Nano GRGC	PL	Hitachi F-4500	150w Xenon Lamp, 320 nm
Long et al. 2019 [102]	GO, rGO	Raman spectroscopy	Renishaw In Via	532 nm Laser
	GO, rGO	TEM	Talos 200F	
	Paste based GRGC	Isothermal Calorimeter	TAM Air	
	Paste based GRGC	XRD	DX 2500	Cu Anode, 40 kV, 40 mA, Range (5-80°C), Rate= 2°/step
	Paste based GRGC	NMR	JEOL, JNM-ECZ-600R/M1	Spinning speed (10.0 kHz), 3.2 mm zirconia rotors,
	Aggregate based GRGC	Flexural Strength	YHZ-300	Loading rate- 500 N/s,
Zhang et al. 2020 [37]	Paste based Nano GRGC	FTIR	Bruker Tensor 27	KBr disk.
	Paste based Nano GRGC	TG, DTG	Mettler Toledo TGA/DSC1	Nitrogen atmosphere
	Paste based Nano GRGC	BET	ASAP 2020	Liquid N_2 (77K)
	Paste based Nano GRGC	Flexural Strength	DKZ-5000	Loading speed (50 N/s)
Zhou et al. 2020 [47]	Ink based GRGC (3D Printed)	Mechanical Properties	UTM AG-IS	Compression speed- 0.5 mm s^{-1}
	Ink based Nano GRGC	SEM	ZEISS merlin compact	
	Ink based GRGC (3D	FTIR	Agilent Cary 660	

	Printed)			
Liu et al. 2020 [84]	Paste based GRGC	XRD	X'Pert PRO MPD	Cu-Kα radiation, Scanning speed (2°/min), Step size (0.002°), Continuous Scan (5°-70°[2θ])
	GO, rGO, Paste based GRGC	FTIR	Nicolet IS 10	Spectral range (4000–650 cm^{-1}), Resolution (4 cm^{-1})
	Paste based GRGC	XPS	Thermo ESCALAB 250XI	Al Kα (0.050 eV), 10 mA, 15 kV
	Paste based GRGC	BET	ASAP 2460	
	Paste based GRGC	SEM-EDS	Hitachi SU8000	
Matalkah et al. 2020 [121]	Paste based GRGC	SEM	JEOL JCM-5000	Gold–Palladium alloy coating, Sputter coater (DESK II), 10 kV
	Paste based GRGC	Isothermal Calorimeter	I-Cal 2000 HPC	
	Paste based GRGC	TGA	Perkin Elmer TGA 4000	
Lertcumfu et al. 2020 [122]	Paste based GRGC	XRD	Rigaku Smartlab	2θ (10°-80°)
	Paste based GRGC	FTIR	Thermo Nicolet Nexus 4700	4000 cm^{-1} - 500 cm^{-1}
	Paste based GRGC	Raman spectroscopy	HORIBA Jobin Yvon T64000	Ar laser, 532 nm, 7.5 mW
	Paste based GRGC	SEM	JSM-IT300	
	Paste based GRGC	UV-Vis Spectrophotometer	Perkin Elmer Lambda 35	
Bellum et al. 2020 [8]	Aggregate based GRGC	SEM	TESCAN VEGA 3 SBH	10 – 30 kV
	Aggregate based GRGC	RCPT (Rapid Chloride Permeability Test)	NRA - 1190	220 - 240v, 50 Hz
Guo et al. 2020 [123]	Paste based Nano GRGC	TEM	Tecnai TF20 FEI	
	Paste based Nano GRGC	AFM	NT-MDT Prima	
	Paste based GRGC	Flexural strength	Pulibang DY208-M20	Speed (50 N/s)
	Paste based GRGC	PSD	Micromeritics Autopore IV 9510	
	Paste based GRGC	SEM	Hitachi JSM-7800F	
Long et al. 2020 [114]	Paste based GRGC	Compressive, Flexural strength	UTM (YZH-300.10)	Loading rate (20 N/s & 2.4 kN/s)
	Paste based GRGC	Thermal Conductivity	XiaTech TC3000	
	Paste based GRGC	SEM	Quanta FEG 250	10 kV
Chougan et al. 2020 [124]	Paste	Rheology	Malvern KinexusLab+	
	Aggregate based GRGC	Compressive, Flexural strength	UTM (Instron 5960)	Loading rate (1 mm/min)
	Source materials, Aggregate based GRGC	SEM/EDS	Carl Zeiss Supra 35VP/EDAX	

4.5. Applications

Potential applications of GRGC have been discussed in the previous publication [111]. Quite a few include structural applications [114], hydrogen production [36], structural supercapacitor [48], and 3D printing [28,47]. GRGC are exceptionally advanced in terms of conventional structural applications owing to their enhanced mechanical properties in different phases. Due to the self-sensing properties of GRGC, they are considered smart composites/materials and thus can be utilized for structural health monitoring applications

[27]. GRGC favors hydrogen production as graphene and the semiconductor metal oxides present in the composite sustain a synergistic effect [36]. Studies have implicated the role of graphene in improving the separation efficiency of photo-excited electrons and holes, thereby enabling photocatalytic water-splitting through solar simulation irradiation. Application as a structural supercapacitor verifies the multifunctionality of GRGC [48]. Higher conductivity of GRGC and extensive pores in the geopolymer matrix offer adequate pathways for ion storage and motion, exhibiting ideal capacitive behaviour. Additive manufacturing methods can accelerate GRGC fabrication and help construct complex frameworks efficiently. Extrusion-based 3D printing of GRGC has been carried out in certain investigations, demonstrating enhanced behaviour as compared to cast-in-mold composites [124]. Recent investigations have revealed compelling results and have paved the way towards a more secure and sustainable future. GRGC is entirely supported by applied sustainability methods and carries a major role in the progression of the construction industry. Major perks of GRGC include industrial waste immobilization, utilization, and lowering of carbon footprint.

5. *Research Gaps and Future Research Directions*

Developing sustainable materials could help in minimizing solid and industrial waste and restoring ecological balance. Geopolymers mostly utilize industrial wastes as source materials and were initially employed as building materials due to their unique properties compared to conventional OPC-based cementitious materials. Reinforcement of the geopolymer composites with GA has broadened the scope of their applications; thereby empowering sustainability and reducing carbon footprint through substituting earlier used conventional materials.

Several research on GRGC has been initiated in recent times (mostly in the last 5 years) which explain the limited number of investigations on the same. Contemporary investigations on GRGC concentrate primarily on methods of production, mechanical and electrical

property improvements, and microstructure characterization of the manufactured composites. Although the results are propitious and encouraging for multiple applications, the practices involved are not extensive. In Particular, this is due to the variability in different graphene derivatives, non-established GA dispersion and mixing protocol, lac of the number of studies and inconsistent result from researchers to researchers, high cost of GA, and limitation in the large-scale field applications of GRGC. For example, while studying the impact of different size GO in the geopolymer composites, small size GO found enhanced the mechanical properties and large size GO improved the rheological behaviour of GRGC in the ink phase [47]. However, studies on the different size GO effect on the GRGC in most cases are very limited, particularly for paste, and aggregate-based GRGC phases. Another factor is the wide dosage of graphene derivatives from 0.00001 to 5 wt.% [19,28,37,101,103] have been used to enhance the mechanical, electrical, photocatalytic, and microstructural properties of GRGC. Then again, the optimized dosage of different types of graphene derivatives is not consistently reported among different studies. Also, the characteristics of different graphene derivatives that dictate their optimum dosage are not comprehensively studied and established. Finally, many studies on GRGC used laboratory-scale production of graphene-based materials with limited detailed characterization, consistent and industrial-scale production of a specific grade of graphene-based materials for geopolymer is going to be a vital challenge.

More efforts are considerably required to bridge the gaps in the production and characterization of GRGC. The effectiveness, economic aspects, and sustainability of GRGC ought to be taken into consideration in its inception stage. Several challenging aspects and research gaps are identified while reviewing existing studies:

- This is not clearly established that which forms, and characteristics of graphene materials are most suitable for specific geopolymer composites.

- No studies reported the performance of geopolymers corresponds to a range of graphene size and content of functional groups.
- The dispersion of GA stands as one of the principal issues in the production of GRGC. Many articles are focused on dispersion techniques, whereas a limited emphasis is given to the dispersion state.
- The R & D of nano-dispersion technologies in geopolymer composites is limited due to the unavailability of diverse dispersion methods which is a major research gap.
- Multiple publications have stated the expedited impact of GA on the geopolymerization process, but not many have characterized the geopolymerization degree.
- Microstructural analysis of GRGC was conducted on most of the relevant studies which reveal some level of understanding of the interplay between the GA and geopolymer matrix. Nevertheless, there are contradictions while a series of articles suggest that GAs do not contribute to the formation of any new additional compounds in the GRGC matrix and others oppose this claim.
- The GRGC specimens have not yet been examined in the concrete configuration in most cases. Besides FA and Metakaolin, not many geopolymer binders have been studied regarding their consistency in GRGC.
- In-depth durability studies on the GRGC are limited in current studies.

A combination of experimental investigation and computational analysis is presumed to advance the GRGC development procedure owing to the complex relationships among numerous experimental parameters. Most of the experimental investigations are focused on mechanical properties while additional investigations are essential to analyze the full potential of the composites. It is implied that the externally attributed stress in GRGC could be adequately redirected to GA for uniform load distribution. Research findings have

indicated that the interfacial stress shear strength regulates the transition of stress to GA. Interfacial transmission of load in GA within the matrix is deemed necessary for effective reinforcing effect. Hence microstructural investigation is required in the direction of understanding complete hydration kinetics, and the influence of different forms and sizes of GAs bonding behaviour with the geopolymer matrix. Additional in-depth investigations are essential to understand the behaviour of GRGC in different environmental conditions and to perceive the less studied properties; thermal, durability, gas barrier, etc. Despite the experimental techniques, modeling methods, namely coarse grain simulation and density functional theory could widen our understanding of GRGC. Besides, worldwide fly ash generation is gradually descending due to the high carbon footprint involved during its generation as a waste byproduct from coal burned power plants. So, competent alternative precursor materials could lead a long way in the development of more sustainable GRGC.

6. Conclusion

The current study offers a comprehensive review of the development of GRGC. Different phases of geopolymer composite show promising performance to become the next generation of sustainable construction material. Despite the fact, geopolymers possess certain limitations such as low flexural and tensile strength, brittleness, and poor impermeability.

Recent investigations show that graphene-based nanomaterials could be used at low loading (<1%) to achieve an enhancement in the microstructural and flexural strength of geopolymer, through the reduction in porosity due to microstructure densification, strong bonding, and mechanical interaction between graphene and geopolymer matrix. To this extent, three different GRGC phases have been studied: ink, paste, and aggregate based composite.

The bibliometric analysis identified the current research trends. Out of the different field of studies with geopolymer, more research trend is noted in the area of structural material

applications, hydrogen production, mechanical properties, electrical properties, and microstructural characterization. The network and keywords density visualization analysis suggest that graphene derivatives such as GO and rGO are used targeting to improve the geopolymerization, hydration kinetics, mechanical properties (compressive and flexural strength, fracture toughness), electrical properties, photocatalytic performance, and microstructure of the graphene composites system.

Typically, graphene derivatives such as GNP, GO and rGO are used to produce GRGC. These graphene derivatives are commonly produced from graphite; GNP through ultrasonication and liquid phase exfoliation, while GO and rGO through different chemical oxidation and reduction process. Pristine graphene has not been a choice for GRGC owing to its high production price and dispersion challenges in the geopolymer matrix. The selection of the types of graphene derivatives depends on the specific properties and how efficiently can be dispersed into the geopolymer matrix. Nevertheless, the commercial scale-up and sustainable production process of graphene derivatives remained a challenging sector to progress.

Efficient dispersion of graphene-based nanomaterials in the geopolymer matrix is identified as the prime factor in the production of geopolymer composites. Graphene derivatives were mixed to produce ink, paste, and aggregate based composite phases at different stages by different researchers, while ultrasonication and mechanical mixing in the solution phase reported more efficient performance. The agglomeration of graphene-based materials in geopolymer matrix is consistently reported as a challenging issue, while more established methods of GRGC production are yet to be developed.

GRGC incorporating very low loadings of graphene additives (<1%) exhibit enhancement in mechanical and electrical properties, as well as the microstructure of the geopolymer matrix. Microcrack bridging obstructing crack propagation in the composite matrix due to graphene

nanoparticles enhances the mechanical properties which can be observed through the microstructural investigations. The use of graphene nanoparticles as a conductive filler in composites indicates exceptional electrical properties as well. However, graphene derivatives with a wide variety of physical properties and chemical characteristics, and mixing process were used to produce GRGC, which results from challenges in the consistent performance enhancement while comparing one study to another. Besides, some published papers use graphene materials from research labs with inconsistent properties without complete characterization which compromise the scientific consistency of the reported results.

Future investigations on GRGC will need to address the current challenges and research gaps, which include specification of suitable forms of graphene derivatives for geopolymer (such as physical size, layer number, functionalization state, dispersion in polar solvents, mechanical and electrical properties), optimum graphene dosage, efficient graphene dispersion, establish mixing protocol, geopolymerisation degree, source materials, and extensive microstructural analysis to get a complete understanding on the behaviour and morphology of the composite. Although the cost of graphene derivatives remains one of the primary barriers for bulk application in geopolymer, this is to some extent acceptable while very low dosages (for example 0.05%) can modify the required properties. On top of it, the production cost of graphene derivatives is expected to be reasonable in the coming times due to research and developments in the industrial scale up graphene production sector.

The GRGC have been investigated in the field of advanced materials application such as structural health monitoring, structural supercapacitor, hydrogen production, 3D printing, dye wastewater degradation, concrete and have exhibited encouraging results. It is foreseeable that the GRGC will be able to aid in the transition from the current linear economy to the circular economy and will have excellent prospects for the future. GRGC also opened great prospects for industrial waste immobilization, utilization, and lowering of carbon footprint. In

order to make full use of the advantages of graphene/geopolymer and produce higher performance building materials, further investigations are essential to overcome existing problems and challenges while bridging current research gaps, requiring further research and exploration. Ultimately, it would lead to areas of study that are explicitly targeted towards the sustainable use of industrial by-products in potential real-world implementations.

Data Availability Statement

No data, models, or code were generated or used during the study.

Acknowledgement

The authors are grateful for Tanvir Qureshi's IFA: New Starters (Faculty funded) award from the University of the West of England, Bristol (UK). The authors are also grateful for the academic support from their affiliate universities, Veer Surendra Sai University of Technology (India), and Texas State University (USA).

References

[1] L. Senff, D. Hotza, S. Lucas, V.M. Ferreira, J.A. Labrincha, Effect of nano-SiO2 and nano-TiO2 addition on the rheological behavior and the hardened properties of cement mortars, Materials Science and Engineering A. 532 (2012) 354–361. https://doi.org/10.1016/j.msea.2011.10.102.

[2] P. Brzozowski, E. Horszczaruk, K. Hrabiuk, The Influence of Natural and Nano-additives on Early Strength of Cement Mortars, Procedia Engineering. 172 (2017) 127–134. https://doi.org/10.1016/j.proeng.2017.02.034.

[3] D.J.M. Flower, J.G. Sanjayan, Green house gas emissions due to concrete manufacture, The International Journal of Life Cycle Assessment. 12 (2007) 282–288. https://doi.org/10.1007/s11367-007-0327-3.

[4] W.P. Zakka, N.H. Abdul Shukor Lim, M. Chau Khun, A scientometric review of geopolymer concrete, Journal of Cleaner Production. 280 (2021) 124353. https://doi.org/10.1016/j.jclepro.2020.124353.

[5] P. Duxson, J.L. Provis, G.C. Lukey, J.S.J. van Deventer, The role of inorganic polymer technology in the development of "green concrete," Cement and Concrete Research. 37 (2007) 1590–1597. https://doi.org/10.1016/j.cemconres.2007.08.018.

[6] J. Davidovits, GEOPOLYMERS: Inorganic polymerie new materials, Journal of Thermal Analysis. 37 (1991) 1633–1656. https://doi.org/10.1007/bf01912193.

[7] P.J. Davidovits, 30 Years of Successes and Failures in Geopolymer Applications . Market Trends and Potential Breakthroughs ., in: Geopolymer 2002 Conference, 2002: pp. 1–16.

[8] R.R. Bellum, K. Muniraj, C.S.R. Indukuri, S.R.C. Madduru, Investigation on Performance Enhancement of Fly ash-GGBFS Based Graphene Geopolymer Concrete, Journal of Building Engineering. 32 (2020) 101659. https://doi.org/10.1016/j.jobe.2020.101659.

[9] M.R. Wang, D.C. Jia, P.G. He, Y. Zhou, Influence of calcination temperature of kaolin on the structure and properties of final geopolymer, Materials Letters. 64 (2010) 2551–2554. https://doi.org/10.1016/j.matlet.2010.08.007.

[10] M. Jafari Nadoushan, A.A. Ramezanianpour, The effect of type and concentration of activators on flowability and compressive strength of natural pozzolan and slag-based geopolymers, Construction and Building Materials. 111 (2016) 337–347. https://doi.org/10.1016/j.conbuildmat.2016.02.086.
[11] E.I. Diaz, E.N. Allouche, S. Eklund, Factors affecting the suitability of fly ash as source material for geopolymers, Fuel. 89 (2010) 992–996. https://doi.org/10.1016/j.fuel.2009.09.012.
[12] F.N. Okoye, J. Durgaprasad, N.B. Singh, Effect of silica fume on the mechanical properties of fly ash based-geopolymer concrete, Ceramics International. 42 (2016) 3000–3006. https://doi.org/10.1016/j.ceramint.2015.10.084.
[13] N. Ye, Y. Chen, J. Yang, S. Liang, Y. Hu, B. Xiao, Q. Huang, Y. Shi, J. Hu, X. Wu, Co-disposal of MSWI fly ash and Bayer red mud using an one-part geopolymeric system, Journal of Hazardous Materials. 318 (2016) 70–78. https://doi.org/10.1016/j.jhazmat.2016.06.042.
[14] R.S. Krishna, F. Shaikh, J. Mishra, G. Lazorenko, A. Kasprzhitskii, Mine tailings-based geopolymers: Properties, applications and industrial prospects, Ceramics International. 47 (2021) 17826–17843. https://doi.org/10.1016/j.ceramint.2021.03.180.
[15] G. Lazorenko, A. Kasprzhitskii, F. Shaikh, R.S. Krishna, J. Mishra, Utilization potential of mine tailings in geopolymers: Physicochemical and environmental aspects, Process Safety and Environmental Protection. 147 (2021) 559–577. https://doi.org/10.1016/j.psep.2020.12.028.
[16] J. Mishra, S.K. Das, R.S. Krishna, B. Nanda, Utilization of ferrochrome ash as a source material for production of geopolymer concrete for a cleaner sustainable environment, Indian Concrete Journal. 94 (2020) 40–49.
[17] J. Mishra, S.K. Das, R.S. Krishna, B. Nanda, S.K. Patro, S.M. Mustakim, Synthesis and characterization of a new class of geopolymer binder utilizing ferrochrome ash (FCA) for sustainable industrial waste management, Materials Today: Proceedings. 33 (2020) 5001–5006. https://doi.org/10.1016/j.matpr.2020.02.832.
[18] Y.S. Wang, Y. Alrefaei, J.G. Dai, Silico-aluminophosphate and alkali-aluminosilicate geopolymers: A comparative review, Frontiers in Materials. 6 (2019). https://doi.org/10.3389/fmats.2019.00106.
[19] N. Ranjbar, M. Mehrali, M. Mehrali, U.J. Alengaram, M.Z. Jumaat, Graphene nanoplatelet-fly ash based geopolymer composites, Cement and Concrete Research. 76 (2015) 222–231. https://doi.org/10.1016/j.cemconres.2015.06.003.
[20] C. Liu, X. Huang, Y.Y. Wu, X. Deng, J. Liu, Z. Zheng, D. Hui, Review on the research progress of cement-based and geopolymer materials modified by graphene and graphene oxide, Nanotechnology Reviews. 9 (2020) 155–169. https://doi.org/10.1515/ntrev-2020-0014.
[21] M. Steinerova, L. Matulova, P. Vermach, J. Kotas, The brittleness and chemical stability of optimized geopolymer composites, Materials. 10 (2017). https://doi.org/10.3390/ma10040396.
[22] P. He, D. Jia, T. Lin, M. Wang, Y. Zhou, Effects of high-temperature heat treatment on the mechanical properties of unidirectional carbon fiber reinforced geopolymer composites, Ceramics International. 36 (2010) 1447–1453. https://doi.org/10.1016/j.ceramint.2010.02.012.
[23] Q. Zheng, B. Han, X. Cui, X. Yu, J. Ou, Graphene-engineered cementitious composites: Small makes a big impact, Nanomaterials and Nanotechnology. 7 (2017) 1–18. https://doi.org/10.1177/1847980417742304.
[24] K.J.D. MacKenzie, M.J. Bolton, Electrical and mechanical properties of aluminosilicate inorganic polymer composites with carbon nanotubes, Journal of Materials Science. 44 (2009) 2851–2857. https://doi.org/10.1007/s10853-009-3377-z.
[25] H. Porwal, S. Grasso, M.J. Reece, Review of graphene-ceramic matrix composites, Advances in Applied Ceramics. 112 (2013) 443–454. https://doi.org/10.1179/174367613X13764308970581.
[26] S. Candamano, E. Sgambitterra, C. Lamuta, L. Pagnotta, S. Chakraborty, F. Crea, Graphene nanoplatelets in geopolymeric systems: A new dimension of nanocomposites, Materials Letters. 236 (2019) 550–553. https://doi.org/10.1016/j.matlet.2018.11.022.
[27] M. Saafi, G. Piukovics, J. Ye, Hybrid graphene/geopolymeric cement as a superionic conductor for structural health monitoring applications, Smart Materials and Structures. 25 (2016). https://doi.org/10.1088/0964-1726/25/10/105018.
[28] J. Zhong, G.X. Zhou, P.G. He, Z.H. Yang, D.C. Jia, 3D printing strong and conductive geo-polymer nanocomposite structures modified by graphene oxide, Carbon. 117 (2017) 421–426. https://doi.org/10.1016/j.carbon.2017.02.102.
[29] M. Saafi, K. Andrew, P.L. Tang, D. McGhon, S. Taylor, M. Rahman, S. Yang, X. Zhou, Multifunctional properties of carbon nanotube/fly ash geopolymeric nanocomposites, Construction and Building Materials. 49 (2013) 46–55. https://doi.org/10.1016/j.conbuildmat.2013.08.007.
[30] M. Saafi, L. Tang, J. Fung, M. Rahman, F. Sillars, J. Liggat, X. Zhou, Graphene/fly ash geopolymeric composites as self-sensing structural materials, Smart Materials and Structures. 23 (2014). https://doi.org/10.1088/0964-1726/23/6/065006.

[31] M. Saafi, L. Tang, J. Fung, M. Rahman, J. Liggat, Enhanced properties of graphene/fly ash geopolymeric composite cement, Cement and Concrete Research. 67 (2015) 292–299. https://doi.org/10.1016/j.cemconres.2014.08.011.
[32] S. Yan, P. He, D. Jia, Z. Yang, X. Duan, S. Wang, Y. Zhou, In situ fabrication and characterization of graphene/geopolymer composites, Ceramics International. 41 (2015) 11242–11250. https://doi.org/10.1016/j.ceramint.2015.05.075.
[33] S. Yan, P. He, D. Jia, X. Duan, Z. Yang, S. Wang, Y. Zhou, Effects of graphene oxide on the geopolymerization mechanism determined by quenching the reaction at intermediate states, RSC Advances. 7 (2017) 13498–13508. https://doi.org/10.1039/c6ra26340b.
[34] Y.J. Zhang, P.Y. He, M.Y. Yang, L. Kang, A new graphene bottom ash geopolymeric composite for photocatalytic H2 production and degradation of dyeing wastewater, International Journal of Hydrogen Energy. 42 (2017) 20589–20598. https://doi.org/10.1016/j.ijhydene.2017.06.156.
[35] Y.J. Zhang, P.Y. He, Y.X. Zhang, H. Chen, A novel electroconductive graphene/fly ash-based geopolymer composite and its photocatalytic performance, Chemical Engineering Journal. 334 (2018) 2459–2466. https://doi.org/10.1016/j.cej.2017.11.171.
[36] Y.J. Zhang, Y.X. Zhang, M.Y. Yang, Synthesis of environment-friendly graphene reinforced slag-based nanocomposite and performance of photocatalytic H2 generation, Ferroelectrics. 522 (2018) 36–44. https://doi.org/10.1080/00150193.2017.1391609.
[37] Y.J. Zhang, P.Y. He, M.Y. Yang, H. Chen, L.C. Liu, Renewable conversion of slag to graphene geopolymer for H2 production and wastewater treatment, Catalysis Today. 355 (2020) 325–332. https://doi.org/10.1016/j.cattod.2019.02.003.
[38] A.K. Geim, K.S. Novoselov, The rise of graphene, Nature Materials. 6 (2007) 183–191. https://doi.org/10.1038/nmat1849.
[39] H. Bai, C. Li, G. Shi, Functional composite materials based on chemically converted graphene, Advanced Materials. 23 (2011) 1089–1115. https://doi.org/10.1002/adma.201003753.
[40] S. Park, R.S. Ruoff, Chemical methods for the production of graphenes, Nature Nanotechnology. 4 (2009) 217–224. https://doi.org/10.1038/nnano.2009.58.
[41] Y. Zhu, S. Murali, W. Cai, X. Li, J.W. Suk, J.R. Potts, R.S. Ruoff, Graphene and graphene oxide: Synthesis, properties, and applications, Advanced Materials. 22 (2010) 3906–3924. https://doi.org/10.1002/adma.201001068.
[42] A.A. Balandin, S. Ghosh, W. Bao, I. Calizo, D. Teweldebrhan, F. Miao, C.N. Lau, Superior thermal conductivity of single-layer graphene, Nano Letters. 8 (2008) 902–907. https://doi.org/10.1021/nl0731872.
[43] X. Du, I. Skachko, A. Barker, E.Y. Andrei, Approaching ballistic transport in suspended graphene, Nature Nanotechnology. 3 (2008) 491–495. https://doi.org/10.1038/nnano.2008.199.
[44] K.I. Bolotin, K.J. Sikes, Z. Jiang, M. Klima, G. Fudenberg, J. Hone, P. Kim, H.L. Stormer, Ultrahigh electron mobility in suspended graphene, Solid State Communications. 146 (2008) 351–355. https://doi.org/10.1016/j.ssc.2008.02.024.
[45] C. Lee, X. Wei, J.W. Kysar, J. Hone, Measurement of the elastic properties and intrinsic strength of monolayer graphene, Science. 321 (2008) 385–388. https://doi.org/10.1126/science.1157996.
[46] R.R. Nair, P. Blake, A.N. Grigorenko, K.S. Novoselov, T.J. Booth, T. Stauber, N.M.R. Peres, A.K. Geim, Fine structure constant defines visual transparency of graphene, Science. 320 (2008) 1308. https://doi.org/10.1126/science.1156965.
[47] G.X. Zhou, C. Li, Z. Zhao, Y.Z. Qi, Z.H. Yang, D.C. Jia, J. Zhong, Y. Zhou, 3D printing geopolymer nanocomposites structure: Graphene oxide size effects on a reactive matrix, Carbon. 164 (2020) 215–223. https://doi.org/10.1016/j.carbon.2020.02.021.
[48] J. Xu, D. Zhang, Multifunctional structural supercapacitor based on graphene and geopolymer, Electrochimica Acta. 224 (2017) 105–112. https://doi.org/10.1016/j.electacta.2016.12.045.
[49] A.B.D. Nandiyanto, M.K. Biddinika, F. Triawan, How Bibliographic Dataset Portrays Decreasing Number of Scientific Publication from Indonesia, Indonesian Journal of Science & Technology. 5 (2020) 154–175. https://doi.org/10.17509/ijost.v5i1.22265.
[50] N.J. van Eck, L. Waltman, Software survey: VOSviewer, a computer program for bibliometric mapping, Scientometrics. 84 (2010) 523–538. https://doi.org/10.1007/s11192-009-0146-3.
[51] A.A. Hamzah, R.S. Selvarajan, B.Y. Majlis, Graphene for biomedical applications: A review, Sains Malaysiana. 46 (2017) 1125–1139. https://doi.org/10.17576/jsm-2017-4607-16.
[52] A. Adetayo, D. Runsewe, Synthesis and Fabrication of Graphene and Graphene Oxide: A Review, Open Journal of Composite Materials. 09 (2019) 207–229. https://doi.org/10.4236/ojcm.2019.92012.
[53] J. Mishra, R.S. Krishna, S.K. Das, S.M. Mustakim, An overview of current research trends on graphene and it's applications, World Scientific News. WSN 132 (2019) 206–219. www.worldscientificnews.com.

[54] L. Tang, L. Zhao, L. Guan, 7 Graphene / Polymer Composite Materials : Processing , Properties and Applications, 2017. https://doi.org/10.1515/9783110574432-007.
[55] L. Lin, B. Deng, J. Sun, H. Peng, Z. Liu, Bridging the Gap between Reality and Ideal in Chemical Vapor Deposition Growth of Graphene, Chemical Reviews. 118 (2018) 9281–9343. https://doi.org/10.1021/acs.chemrev.8b00325.
[56] D. Li, M.B. Müller, S. Gilje, R.B. Kaner, G.G. Wallace, Processable aqueous dispersions of graphene nanosheets, Nature Nanotechnology. 3 (2008) 101–105. https://doi.org/10.1038/nnano.2007.451.
[57] Y. Hernandez, V. Nicolosi, M. Lotya, F.M. Blighe, Z. Sun, S. De, I.T. McGovern, B. Holland, M. Byrne, Y.K. Gun'ko, J.J. Boland, P. Niraj, G. Duesberg, S. Krishnamurthy, R. Goodhue, J. Hutchison, V. Scardaci, A.C. Ferrari, J.N. Coleman, High-yield production of graphene by liquid-phase exfoliation of graphite, Nature Nanotechnology. 3 (2008) 563–568. https://doi.org/10.1038/nnano.2008.215.
[58] K.R. Paton, E. Varrla, C. Backes, R.J. Smith, U. Khan, A. O'Neill, C. Boland, M. Lotya, O.M. Istrate, P. King, T. Higgins, S. Barwich, P. May, P. Puczkarski, I. Ahmed, M. Moebius, H. Pettersson, E. Long, J. Coelho, S.E. O'Brien, E.K. McGuire, B.M. Sanchez, G.S. Duesberg, N. McEvoy, T.J. Pennycook, C. Downing, A. Crossley, V. Nicolosi, J.N. Coleman, Scalable production of large quantities of defect-free few-layer graphene by shear exfoliation in liquids, Nature Materials. 13 (2014) 624–630. https://doi.org/10.1038/nmat3944.
[59] R.K. Singh, R. Kumar, D.P. Singh, Graphene oxide: Strategies for synthesis, reduction and frontier applications, RSC Advances. 6 (2016) 64993–65011. https://doi.org/10.1039/c6ra07626b.
[60] B.C. Brodie, On the Atomic Weight of Graphite, Philosophical Transactions of the Royal Society B: Biological Sciences. (1859) 249–259. http://rstb.royalsocietypublishing.org/cgi/doi/10.1098/rstb.1983.0080.
[61] L. Staudenmaier, Method for the preparation of graphitic acid, European Journal of Inorganic Chemistry. 31 (1898) 1481–1487.
[62] W.S. Hummers, R.E. Offeman, Preparation of Graphitic Oxide, Journal of the American Chemical Society. 80 (1958) 1339. https://doi.org/10.1021/ja01539a017.
[63] D.C. Marcano, D. v. Kosynkin, J.M. Berlin, A. Sinitskii, Z. Sun, A. Slesarev, L.B. Alemany, W. Lu, J.M. Tour, Improved synthesis of graphene oxide, ACS Nano. 4 (2010) 4806–4814. https://doi.org/10.1021/nn1006368.
[64] S. Wang, S. Zhang, Y. Wang, X. Sun, K. Sun, Reduced graphene oxide/carbon nanotubes reinforced calcium phosphate cement, Ceramics International. 43 (2017) 13083–13088. https://doi.org/10.1016/j.ceramint.2017.06.196.
[65] H. Yu, B. Zhang, C. Bulin, R. Li, R. Xing, High-efficient Synthesis of Graphene Oxide Based on Improved Hummers Method, Scientific Reports. 6 (2016) 1–7. https://doi.org/10.1038/srep36143.
[66] R. Muzyka, S. Drewniak, T. Pustelny, M. Chrubasik, G. Gryglewicz, Characterization of graphite oxide and reduced graphene oxide obtained from different graphite precursors and oxidized by different methods using Raman spectroscopy, Materials. 11 (2018) 15–17. https://doi.org/10.3390/ma11071050.
[67] S. Pei, Q. Wei, K. Huang, H.M. Cheng, W. Ren, Green synthesis of graphene oxide by seconds timescale water electrolytic oxidation, Nature Communications. 9 (2018) 1–9. https://doi.org/10.1038/s41467-017-02479-z.
[68] P. Ranjan, S. Agrawal, A. Sinha, T.R. Rao, J. Balakrishnan, A.D. Thakur, A Low-Cost Non-explosive Synthesis of Graphene Oxide for Scalable Applications, Scientific Reports. 8 (2018) 1–13. https://doi.org/10.1038/s41598-018-30613-4.
[69] J.A.V. Piñas, T.S. Andrade, A.T. Oliveira, P.E.A. Salomão, M. Rodriguez, A.C. Silva, H.S. Oliveira, D.S. Monteiro, M.C. Pereira, Production of reduced graphene oxide platelets from graphite flakes using the Fenton reaction as an alternative to harmful oxidizing agents, Journal of Nanomaterials. 2019 (2019). https://doi.org/10.1155/2019/5736563.
[70] A.T. Habte, D.W. Ayele, M. Hu, Synthesis and Characterization of Reduced Graphene Oxide (rGO) Started from Graphene Oxide (GO) Using the Tour Method with Different Parameters, Advances in Materials Science and Engineering. 2019 (2019). https://doi.org/10.1155/2019/5058163.
[71] C.K. Chua, M. Pumera, Chemical reduction of graphene oxide: A synthetic chemistry viewpoint, Chemical Society Reviews. 43 (2014) 291–312. https://doi.org/10.1039/c3cs60303b.
[72] S.H. Huh, Thermal Reduction of Graphene Oxide, InTech, 2011. https://doi.org/10.5772/14156.
[73] D. Voiry, J. Yang, J. Kupferberg, R. Fullon, C. Lee, H.Y. Jeong, H.S. Shin, M. Chhowalla, High-quality graphene via microwave reduction of solution-exfoliated graphene oxide, Science. 353 (2016) 1413–1416. https://doi.org/10.1126/science.aah3398.
[74] Y.L. Zhang, L. Guo, H. Xia, Q.D. Chen, J. Feng, H.B. Sun, Photoreduction of Graphene Oxides: Methods, Properties, and Applications, Advanced Optical Materials. 2 (2014) 10–28. https://doi.org/10.1002/adom.201300317.
[75] S. Pei, H.M. Cheng, The reduction of graphene oxide, Carbon. 50 (2012) 3210–3228.

https://doi.org/10.1016/j.carbon.2011.11.010.
[76] S. Dubin, S. Gilje, K. Wang, V.C. Tung, K. Cha, A.S. Hall, J. Farrar, R. Varshneya, Y. Yang, R.B. Kaner, A one-step, solvothermal reduction method for producing reduced graphene oxide dispersions in organic solvents, ACS Nano. 4 (2010) 3845–3852. https://doi.org/10.1021/nn100511a.
[77] Y. Zhou, Q. Bao, L.A.L. Tang, Y. Zhong, K.P. Loh, Hydrothermal dehydration for the "green" reduction of exfoliated graphene oxide to graphene and demonstration of tunable optical limiting properties, Chemistry of Materials. 21 (2009) 2950–2956. https://doi.org/10.1021/cm9006603.
[78] S. Pei, J. Zhao, J. Du, W. Ren, H.M. Cheng, Direct reduction of graphene oxide films into highly conductive and flexible graphene films by hydrohalic acids, Carbon. 48 (2010) 4466–4474. https://doi.org/10.1016/j.carbon.2010.08.006.
[79] D.A. Sokolov, K.R. Shepperd, T.M. Orlando, Formation of graphene features from direct laser-induced reduction of graphite oxide, Journal of Physical Chemistry Letters. 1 (2010) 2633–2636. https://doi.org/10.1021/jz100790y.
[80] M. Baraket, S.G. Walton, Z. Wei, E.H. Lock, J.T. Robinson, P. Sheehan, Reduction of graphene oxide by electron beam generated plasmas produced in methane/argon mixtures, Carbon. 48 (2010) 3382–3390. https://doi.org/10.1016/j.carbon.2010.05.031.
[81] Z. Wang, X. Zhou, J. Zhang, F. Boey, H. Zhang, Direct electrochemical reduction of single-layer graphene oxide and subsequent functionalization with glucose oxidase, Journal of Physical Chemistry C. 113 (2009) 14071–14075. https://doi.org/10.1021/jp906348x.
[82] W. Gao, L.B. Alemany, L. Ci, P.M. Ajayan, New insights into the structure and reduction of graphite oxide, Nature Chemistry. 1 (2009) 403–408. https://doi.org/10.1038/nchem.281.
[83] M. Pfaffeneder-Kmen, I.F. Casas, A. Naghilou, G. Trettenhahn, W. Kautek, A Multivariate Curve Resolution evaluation of an in-situ ATR-FTIR spectroscopy investigation of the electrochemical reduction of graphene oxide, Electrochimica Acta. 255 (2017) 160–167. https://doi.org/10.1016/j.electacta.2017.09.124.
[84] X. Liu, Y. Wu, M. Li, J. Jiang, L. Guo, W. Wang, W. Zhang, Z. Zhang, P. Duan, Effects of graphene oxide on microstructure and mechanical properties of graphene oxide-geopolymer composites, Construction and Building Materials. 247 (2020) 118544. https://doi.org/10.1016/j.conbuildmat.2020.118544.
[85] S.M. Kang, S. Park, D. Kim, S.Y. Park, R.S. Ruoff, H. Lee, Simultaneous reduction and surface functionalization of graphene oxide by mussel-inspired chemistry, Advanced Functional Materials. 21 (2011) 108–112. https://doi.org/10.1002/adfm.201001692.
[86] S. Zhang, Y. Shao, H. Liao, M.H. Engelhard, G. Yin, Y. Lin, Polyelectrolyte-induced reduction of exfoliated graphite oxide: A facile route to synthesis of soluble graphene nanosheets, ACS Nano. 5 (2011) 1785–1791. https://doi.org/10.1021/nn102467s.
[87] X. Shen, L. Jiang, Z. Ji, J. Wu, H. Zhou, G. Zhu, Stable aqueous dispersions of graphene prepared with hexamethylenetetramine as a reductant, Journal of Colloid and Interface Science. 354 (2011) 493–497. https://doi.org/10.1016/j.jcis.2010.11.037.
[88] J. Che, L. Shen, Y. Xiao, A new approach to fabricate graphene nanosheets in organic medium: Combination of reduction and dispersion, Journal of Materials Chemistry. 20 (2010) 1722–1727. https://doi.org/10.1039/b922667b.
[89] Y. Si, E.T. Samulski, Synthesis of water soluble graphene, Nano Letters. 8 (2008) 1679–1682. https://doi.org/10.1021/nl080604h.
[90] G. Wang, J. Yang, J. Park, X. Gou, B. Wang, H. Liu, J. Yao, Facile Synthesis and Characterization of Graphene Nanosheets, The Journal of Physical Chemistry C. 112 (2008) 8192–8195. https://doi.org/10.1021/jp710931h.
[91] Z. Fan, K. Wang, T. Wei, J. Yan, L. Song, B. Shao, An environmentally friendly and efficient route for the reduction of graphene oxide by aluminum powder, Carbon. 48 (2010) 1686–1689. https://doi.org/10.1016/j.carbon.2009.12.063.
[92] M.J. Ferna´ndez-Merino, J.I.P. L. Guardia, S. Villar-Rodil, P. Solı´s-Ferna´ndez, A. Martı´nez-Alonso, J.M.D. Tasco´n, Vitamin C Is an Ideal Substitute for Hydrazine in the Reduction of Graphene Oxide Suspensions, J. Phys. Chem. 114 (2010) 6426–6432. https://doi.org/10.1021/jp100603h.
[93] M. Agharkar, S. Kochrekar, S. Hidouri, M.A. Azeez, Trends in green reduction of graphene oxides, issues and challenges: A review, Materials Research Bulletin. 59 (2014) 323–328. https://doi.org/10.1016/j.materresbull.2014.07.051.
[94] S. Iravani, Green synthesis of metal nanoparticles using plants, Green Chemistry. 13 (2011) 2638–2650. https://doi.org/10.1039/c1gc15386b.
[95] X. Zhou, J. Zheng, H. Wu, H. Yang, J. Zhang, S. Guo, Reducing graphene oxide via hydroxylamine: A simple and efficient route to graphene, Journal of Physical Chemistry C. 115 (2011) 11957–11961. https://doi.org/10.1021/jp202575j.

[96] N.S. Ahmed, O. Azizi, A. El-Boher, J. Gahl, S. Bok, Facile Synthesis and Characterization of Reduced Graphene Oxide Produced with Green and Conventional Reductants, ECS Journal of Solid State Science and Technology. 7 (2018) M173–M179. https://doi.org/10.1149/2.0181811jss.
[97] M.J.Y. Tai, W.W. Liu, C.S. Khe, N.M.S. Hidayah, Y.P. Teoh, C.H. Voon, H.C. Lee, P.Y.P. Adelyn, Green synthesis of reduced graphene oxide using green tea extract, AIP Conference Proceedings. 2045 (2018). https://doi.org/10.1063/1.5080845.
[98] K. Tadyszak, J.K. Wychowaniec, J. Litowczenko, Biomedical applications of graphene-based structures, Nanomaterials. 8 (2018) 1–20. https://doi.org/10.3390/nano8110944.
[99] L.W. Zhang, M.F. Kai, X.H. Chen, Si-doped graphene in geopolymer: Its interfacial chemical bonding, structure evolution and ultrastrong reinforcing ability, Cement and Concrete Composites. 109 (2020) 103522. https://doi.org/10.1016/j.cemconcomp.2020.103522.
[100] S. Guo, X. Qiao, T. Zhao, Y.-S. Wang, Preparation of Highly Dispersed Graphene and Its Effect on the Mechanical Properties and Microstructures of Geopolymer, Journal of Materials in Civil Engineering. 32 (2020) 04020327. https://doi.org/10.1061/(asce)mt.1943-5533.0003424.
[101] G. Zhang, J. Lu, Experimental research on the mechanical properties of graphene geopolymer, AIP Advances. 8 (2018). https://doi.org/10.1063/1.5020547.
[102] W.J. Long, T.H. Ye, Q.L. Luo, Y. Wang, L. Mei, Reinforcing mechanism of reduced graphene oxide on flexural strength of geopolymers: A synergetic analysis of hydration and chemical composition, Nanomaterials. 9 (2019). https://doi.org/10.3390/nano9121723.
[103] G. Xu, J. Zhong, X. Shi, Influence of graphene oxide in a chemically activated fly ash, Fuel. 226 (2018) 644–657. https://doi.org/10.1016/j.fuel.2018.04.033.
[104] A. Amri, Y.B. Hendri, Zultiniar, E. Malindo, M.M. Rahman, Graphene Nanosheets (GNs) Addition on the Palm Oil Fuel Ash (POFA) Based Geopolymer with KOH Activator, Journal of Physics: Conference Series. 1351 (2019). https://doi.org/10.1088/1742-6596/1351/1/012101.
[105] Z. Lu, A. Hanif, C. Ning, H. Shao, R. Yin, Z. Li, Steric stabilization of graphene oxide in alkaline cementitious solutions: Mechanical enhancement of cement composite, Materials and Design. 127 (2017) 154–161. https://doi.org/10.1016/j.matdes.2017.04.083.
[106] Z. Lu, D. Hou, A. Hanif, W. Hao, G. Sun, Z. Li, Comparative evaluation on the dispersion and stability of graphene oxide in water and cement pore solution by incorporating silica fume, Cement and Concrete Composites. 94 (2018) 33–42. https://doi.org/10.1016/j.cemconcomp.2018.08.011.
[107] S. Yan, P. He, D. Jia, Z. Yang, X. Duan, S. Wang, Y. Zhou, Effect of reduced graphene oxide content on the microstructure and mechanical properties of graphene–geopolymer nanocomposites, Ceramics International. 42 (2016) 752–758. https://doi.org/10.1016/j.ceramint.2015.08.176.
[108] T.S. Qureshi, D.K. Panesar, Impact of graphene oxide and highly reduced graphene oxide on cement based composites, Construction and Building Materials. 206 (2019) 71–83. https://doi.org/10.1016/j.conbuildmat.2019.01.176.
[109] S. Yan, P. He, D. Jia, X. Duan, Z. Yang, S. Wang, Y. Zhou, Crystallization kinetics and microstructure evolution of reduced graphene oxide/geopolymer composites, Journal of the European Ceramic Society. 36 (2016) 2601–2609. https://doi.org/10.1016/j.jeurceramsoc.2016.03.026.
[110] J.T. Robinson, F.K. Perkins, E.S. Snow, Z. Wei, P.E. Sheehan, Reduced graphene oxide molecular sensors, Nano Letters. 8 (2008) 3137–3140. https://doi.org/10.1021/nl8013007.
[111] S. Bi, M. Liu, J. Shen, X.M. Hu, L. Zhang, Ultrahigh Self-Sensing Performance of Geopolymer Nanocomposites via Unique Interface Engineering, ACS Applied Materials and Interfaces. 9 (2017) 12851–12858. https://doi.org/10.1021/acsami.7b00419.
[112] S. Yan, P. He, D. Jia, X. Duan, Z. Yang, S. Wang, Y. Zhou, P. Colombo, In Situ Processing of Graphene/Leucite Nanocomposite Through Graphene Oxide/Geopolymer, Journal of the American Ceramic Society. 99 (2016) 1164–1173. https://doi.org/10.1111/jace.14089.
[113] S. Yan, P. He, D. Jia, X. Duan, Z. Yang, S. Wang, Y. Zhou, In-situ preparation of fully stabilized graphene/cubic-leucite composite through graphene oxide/geopolymer, Materials and Design. 101 (2016) 301–308. https://doi.org/10.1016/j.matdes.2016.03.139.
[114] W.J. Long, C. Lin, X.W. Tan, J.L. Tao, T.H. Ye, Q.L. Luo, Structural applications of thermal insulation alkali activated materials with reduced graphene oxide, Materials. 13 (2020). https://doi.org/10.3390/ma13051052.
[115] S. Yan, P. He, D. Jia, Z. Yang, X. Duan, S. Wang, Y. Zhou, Effects of treatment temperature on the reduction of GO under alkaline solution during the preparation of graphene/geopolymer composites, Ceramics International. 42 (2016) 18181–18188. https://doi.org/10.1016/j.ceramint.2016.08.134.
[116] T.S. Qureshi, D.K. Panesar, B. Sidhureddy, A. Chen, P.C. Wood, Nano-cement composite with graphene oxide produced from epigenetic graphite deposit, Composites Part B: Engineering. 159 (2019) 248–258. https://doi.org/10.1016/j.compositesb.2018.09.095.
[117] T.S. Qureshi, D.K. Panesar, Nano reinforced cement paste composite with functionalized graphene and

pristine graphene nanoplatelets, Composites Part B: Engineering. 197 (2020) 108063. https://doi.org/10.1016/j.compositesb.2020.108063.
[118] X. Fan, W. Peng, Y. Li, X. Li, S. Wang, G. Zhang, F. Zhang, Deoxygenation of exfoliated graphite oxide under alkaline conditions: a green route to graphene preparation, Advanced Materials. 20 (2008) 4490–4493. https://doi.org/10.1002/adma.200801306.
[119] H.R. Thomas, C. Vallés, R.J. Young, I.A. Kinloch, N.R. Wilson, J.P. Rourke, Identifying the fluorescence of graphene oxide, Journal of Materials Chemistry C. 1 (2013) 338–342. https://doi.org/10.1039/c2tc00234e.
[120] Y.J. Zhang, M.Y. Yang, L. Zhang, K. Zhang, L. Kang, A new graphene/geopolymer nanocomposite for degradation of dye wastewater, Integrated Ferroelectrics. 171 (2016) 38–45. https://doi.org/10.1080/10584587.2016.1171178.
[121] F. Matalkah, P. Soroushian, Graphene nanoplatelet for enhancement the mechanical properties and durability characteristics of alkali activated binder, Construction and Building Materials. 249 (2020) 118773. https://doi.org/10.1016/j.conbuildmat.2020.118773.
[122] N. Lertcumfu, P. Jaita, S. Thammarong, S. Lamkhao, S. Tandorn, C. Randorn, T. Tunkasiri, G. Rujijanagul, Influence of graphene oxide additive on physical, microstructure, adsorption, and photocatalytic properties of calcined kaolinite-based geopolymer ceramic composites, Colloids and Surfaces A: Physicochemical and Engineering Aspects. 602 (2020) 125080. https://doi.org/10.1016/j.colsurfa.2020.125080.
[123] S. Guo, X. Qiao, T. Zhao, Y.-S. Wang, Preparation of Highly Dispersed Graphene and Its Effect on the Mechanical Properties and Microstructures of Geopolymer, Journal of Materials in Civil Engineering. 32 (2020) 04020327. https://doi.org/10.1061/(asce)mt.1943-5533.0003424.
[124] M. Chougan, S. Hamidreza Ghaffar, M. Jahanzat, A. Albar, N. Mujaddedi, R. Swash, The influence of nano-additives in strengthening mechanical performance of 3D printed multi-binder geopolymer composites, Construction and Building Materials. 250 (2020) 118928. https://doi.org/10.1016/j.conbuildmat.2020.118928.